

Notes on the dynamics of noncommutative $U(2)$ and commutative $SU(3)$ instantons

Douglas J. Smith,^{*} Calum J. Robson,[†] and Joseph A. Farrow[‡]

Department of Mathematical Sciences, Durham University, Durham DH1 3LE, United Kingdom



(Received 17 May 2022; accepted 9 June 2022; published 1 August 2022)

We examine the dynamics of noncommutative instantons of instanton number 2 and commutative instantons of instanton number 3 in 5D super Yang-Mills theory. We begin by detailing the construction of the 1/4-Bogomolyni-Prasad-Somerfeldt instanton solutions, their moduli space, and the moduli space potential using an explicit parametrization of the moduli space coordinates in terms of the biquaternions. We then go on to numerically analyze the dynamics on the moduli spaces we have constructed, discussing some of the numerical issues which arose, and describing the numerical algorithm we developed to solve them.

DOI: [10.1103/PhysRevD.106.045001](https://doi.org/10.1103/PhysRevD.106.045001)

I. INTRODUCTION

The aim of this paper is to present new solutions for the moduli space dynamics of 2- and 3-instantons in 5D super Yang-Mills (SYM) theory. Instantons are a specific example of topological solitons, which are nonlinear solutions to certain partial differential equations (PDEs). Because the properties of these solutions are tied to topological invariants of the spaces they are defined upon, they are very stable—no continuous transformation (including time evolution) of the solutions can cause these properties to change. Originally discovered in [1], research into their properties took off after the discovery of the Atiyah-Drinfeld-Hitchin-Manin (ADHM) method for constructing them in [2]. Whilst instantons were originally constructed as solutions in four Euclidean dimensions, we can also define them in 5D SYM. Here the instantons are static solutions in every slice of the four Euclidean dimensions, and the 5th timelike dimension is seen as describing their evolution. In the context of string theory this arises since the instantons appear as 1/2-Bogomolyni-Prasad-Somerfeldt (BPS) states corresponding to an interacting system of D0-branes and D4-branes [3,4].

In this system, there are five $SU(N)$ scalar fields which describe the transverse positions of the D4-branes. Separating the branes gives at least one of these scalars a nonzero expectation value. In the low-energy limit this corresponds to introducing a nonzero scalar field on top of

the instanton equations. This configuration would usually be an unstable field configuration due to interactions with the Higgs field; however, the introduction of the scalar field gives the instantons an electric charge which balances the scalar Higgs field, producing a stable solution [5,6]. These charged instantons are known as dyonic instantons, and are 1/4-BPS rather than 1/2-BPS. They are the low-energy limits of a bound state of fundamental strings and D0-branes.

This system has been the subject of particular interest as the low-energy limit of M5 branes in M-Theory. The low-energy dynamics of these objects is described using the so-called (2,0) theory, a 6D superconformal field theory. It has been shown that if we dimensionally reduce this theory, we get 5D SYM [7,8]. Another way of reducing the number of dimensions is to compactify one of the six dimensions into an S^1 . Somewhat surprisingly, it turns out that this also gives 5D SYM theory. In this case, the instanton sector, with separate solutions labeled by the integer instanton number k , has been shown to agree for low k with the Kaluza-Klein modes arising from the compactification, which are labeled by an integer winding number. This raises the possibility that if these sectors are in fact identical, then 5D SYM with all instantons included corresponds to including all the Kaluza-Klein modes of the compactified (2,0) theory. This would imply that the 6D (2,0) theory is the UV fixed point of 5D SYM, even though 5D SYM is perturbatively nonrenormalizable [9,10].

Directly calculating the dynamic behavior of instanton solutions is both analytically and computationally expensive. The moduli space method developed by Manton [11] simplifies things by treating the free parameters as coordinates on a manifold, called the moduli space. Evolution of an instanton solution is approximated for slow motion by geodesic motion on the moduli space. This moduli space contains singularities when the size of the instanton shrinks to zero size. They correspond in the string theory to

^{*}douglas.smith@durham.ac.uk

[†]c.j.robson@lse.ac.uk

[‡]joseph.a.farrow@durham.ac.uk

Published by the American Physical Society under the terms of the [Creative Commons Attribution 4.0 International license](https://creativecommons.org/licenses/by/4.0/). Further distribution of this work must maintain attribution to the author(s) and the published article's title, journal citation, and DOI. Funded by SCOAP³.

a transition between the Coloumb and Higgs branches of the D0 theory [4].

This is the motivation for introducing noncommutativity, corresponding to adding a Fayet-Illiopoulos term to the string theory. Defining the instantons on a noncommutative spacetime has the effect of introducing a minimum size for the instantons. This resolves the moduli space singularities as the instantons can only shrink to a finite size, so cannot reach the singularity where their size vanishes.

We begin by introducing instantons themselves, and the noncommutative spacetimes we will be studying them on. This includes a brief discussion of the biquaternions—the algebra $\mathbb{C} \times \mathbb{H}$. The calculation of instanton solutions uses the ADHM construction first developed in [2]. We briefly review the use of this method in the $SU(2)$ Yang-Mills case.

We then introduce the instanton moduli space [11]. We recap how this construction can be extended to dyonic instantons via introducing a potential on the moduli space, following the presentation in [12]. A practical method for calculating the moduli space metric and potential for noncommutative $U(N)$ instantons is presented in Appendix C. This generalizes the method presented for $SU(2)$ commutative instantons in [13].

In the second part of the paper, we look for solutions to the equations we have derived. The noncommutative two-instanton case was first studied in [14] however we found an error in this result. We were unable to find the exact result for the full moduli space but we present a solution defined on a subspace of the full moduli space taking values in the $\mathbb{C} \times \mathbb{C}$ subgroup of $\mathbb{C} \times \mathbb{H}$; this is a geodesic submanifold of the full moduli space. After finding this solution, we use it to derive the metric and potential on this subspace. We then numerically evaluate scattering in this subspace and we compare these results to the results for the commutative two-instanton in [13].

Finally, we look at the commutative three-instanton case. Again we present a solution for the complex subspace $\mathbb{C} \times \mathbb{C}$ and calculate the moduli space metric and potential for that subspace. Numerical scattering calculations proved to be very computationally expensive; however, we were able to plot scalar field and topological charge density profiles, which allowed us to make some comparison to the two-instanton case in the appropriate limits.

We use two different numerical algorithms to integrate the moduli space equation of motion, depending on the algebraic complexity of the moduli space metrics and potentials considered. For two noncommutative instantons with an orthogonal gauge embedding and four-dimensional moduli space, we find the system sufficiently simple to solve with the numerical algorithm developed in [13]. Increasing to the full six-dimensional gauge embedding results in significantly more complex metrics and potentials on the moduli space, and we find that these cases are no longer tractable to the algorithm from [13]. To overcome this problem we developed a new numerical algorithm.

II. BACKGROUND MATERIAL

We begin by defining our notations and conventions for the biquaternions and for noncommutative spacetime. These will be used throughout the rest of the paper.

A. Quaternions and biquaternions

The group $\mathbb{C} \times \mathbb{H}$, known as complex quaternions, biquaternions, and even tessarions has a long history [15]. To avoid confusion we will refer to the group as biquaternions in the rest of the paper. As discussed in, e.g., [16], the algebra is equipped with three notions of conjugation. We write a general element of the group as

$$q = q_R + iq_I = q_{R0} + \mathbf{q}_R + i(q_{I0} + i\mathbf{q}_I). \quad (1)$$

Where $q_R, q_I \in \mathbb{H}$, and correspondingly $q_{R0}, q_{I0} \in \mathbb{R}$ and $\mathbf{q}_R, \mathbf{q}_I$ belong to the quaternion imaginary part of \mathbb{H} . Then we have a complex conjugation q^* , which takes

$$q_R + iq_I \rightarrow q_R - iq_I. \quad (2)$$

We also have a quaternion conjugation \bar{q}

$$q_R + iq_I \rightarrow \bar{q}_R + i\bar{q}_I = q_{R0} - \mathbf{q}_R + i(q_{I0} - \mathbf{q}_I). \quad (3)$$

Finally, we have a total conjugation q^\dagger which applies both these operations simultaneously

$$q_R + iq_I \rightarrow \bar{q}_R - i\bar{q}_I = q_{R0} - \mathbf{q}_R - i(q_{I0} - \mathbf{q}_I). \quad (4)$$

To clarify our notation, we use the basis σ_n for the quaternions, with $\sigma_n = (\mathbb{1}_2, i\tau_i)$, where the τ_i are the standard Pauli matrices. We also define $\bar{\sigma}_n = (\mathbb{1}_2, -i\tau_i)$. Further, we define the self-dual object

$$\sigma_{mn} = \frac{1}{4}(\sigma_m \bar{\sigma}_n - \sigma_n \bar{\sigma}_m), \quad (5)$$

and the antiself-dual

$$\bar{\sigma}_{mn} = \frac{1}{4}(\bar{\sigma}_m \sigma_n - \bar{\sigma}_n \sigma_m). \quad (6)$$

Here, we define a self-dual matrix as one for which $A_{nm}^* = A_{mn}$, and an antiself-dual one as $A_{nm}^* = -A_{mn}$. With these definitions, we have

$$\begin{aligned} \sigma_0 &= \begin{bmatrix} 1 & 0 \\ 0 & 1 \end{bmatrix}, & \sigma_1 &= \begin{bmatrix} 0 & -1 \\ 1 & 0 \end{bmatrix}, \\ \sigma_2 &= \begin{bmatrix} 0 & i \\ i & 0 \end{bmatrix}, & \sigma_3 &= \begin{bmatrix} i & 0 \\ 0 & -i \end{bmatrix}. \end{aligned} \quad (7)$$

Finally, the fact that the biquaternions have multiple notions of conjugation means that there are multiple

notions of the imaginary part. We will use $\text{Im}_{\mathbb{H}}$ to denote the quaternion imaginary part, defined for $q = q_0 + \mathbf{q} \in \mathbb{H}$, with $q_0 \in \mathbb{R}$ and \mathbf{q} a purely imaginary quaternion, as

$$\text{Im}_{\mathbb{H}}(q) = \mathbf{q}. \quad (8)$$

We also have the complex imaginary part, defined for $z \in \mathbb{C}$, $z = x + iy$ as

$$\text{Im}_{\mathbb{C}}(z) = y. \quad (9)$$

Note that $\text{Im}_{\mathbb{C}}$ doesn't include the factor i which we must add in by hand where it is required—this is done to match with the usual definition of Im in the complex case. However it does mean some care has to be taken when restricting from \mathbb{H} to \mathbb{C} , as i then corresponds to the imaginary quaternion basis vector, which is included in $\text{Im}_{\mathbb{H}}$ but not in $\text{Im}_{\mathbb{C}}$.

In the case of a biquaternion $q = q_R + iq_I$ we have

$$\text{Im}_{\mathbb{C}}(q) = q_I; \quad \text{Im}_{\mathbb{H}}(q) = \mathbf{q}_R + i\mathbf{q}_I, \quad (10)$$

where \mathbf{q}_R and \mathbf{q}_I are the quaternion imaginary parts of q_R and q_I respectively. We similarly define $\text{Re}_{\mathbb{H}}$ and $\text{Re}_{\mathbb{C}}$.

B. Noncommutativity

It is convenient to introduce the study of noncommutative spacetimes into the study of instantons. It is convenient because it allows us to resolve singularities on the instanton moduli space (see the next section). It was first shown in [17] that this was possible, and since then many examples have been constructed (see e.g., [18–20] for a selection).

To construct a noncommutative version of \mathbb{R}^4 , we simply impose an anticommutation relation on the spacetime coordinates

$$[x^m, x^n] = \theta^{mn}. \quad (11)$$

Here m, n are the Euclidean-Lorentz indices, and θ^{mn} is a real, antisymmetric, constant matrix. We can always rotate it into the form

$$\theta^{mn} = \begin{bmatrix} 0 & \theta^{12} & 0 & 0 \\ -\theta^{12} & 0 & 0 & 0 \\ 0 & 0 & 0 & \theta^{34} \\ 0 & 0 & -\theta^{34} & 0 \end{bmatrix}. \quad (12)$$

There are several interesting subcases of this matrix [20]; in this paper we consider the self-dual (SD) case, where $\theta^{12} = \theta^{34} = 2\zeta$.

The noncommutativity of the spacetime coordinates forces us to modify our notion of the multiplication of functions. Rather than the usual multiplication, we use the *Moyal Star Product* [21]. This is defined as

$$f(x) \star g(x) = \exp\left(\frac{i}{2}\theta^{ij}\partial_i\partial_j\right)f(x)g(x)|_{x=x'}. \quad (13)$$

This gives the following expansion on powers of θ^{ij}

$$f(x) \star g(x) = f(x)g(x) + \frac{i}{2}\theta^{ij}\partial_i f(x)\partial_j g(x) + \mathcal{O}(\theta^2). \quad (14)$$

Using this, the gauge potential and field strength become

$$A_i \rightarrow g^{-1} \star A_i \star g + g^{-1} \star \partial_i g, \quad (15)$$

and

$$F_{ij} = \partial_{[i}A_{j]} - i[A_i, A_j]_{\star}, \quad (16)$$

where

$$[A_i, A_j]_{\star} = A_i \star A_j - A_j \star A_i. \quad (17)$$

This has two effects on our instanton solutions. First of all, it allows us to find solutions with no commutative equivalent, since the additional length scale $[\zeta] = [\text{length}]^2$ and the fact we are not in Euclidean flat space means Derrick's theorem does not apply.

Secondly, and less positively, in theory it implies we have an infinite number of terms to calculate. However, we can avoid this thanks to an isomorphism between the algebra of functions with the \star -product, and certain operators over Hilbert space. This is more fully discussed in [22].

III. DYONIC INSTANTONS

Now we have discussed these notational conventions we define what is meant by dyonic instantons. Following the presentation in [13] we start with the action

$$S_{\text{YM}} = \int d^5x \frac{1}{4} F_{\mu\nu}^a F_a^{\mu\nu} + \frac{1}{2} D_{\mu}\phi D^{\mu}\phi. \quad (18)$$

We consider static solutions, for which the integral is taken over the four spatial dimensions. These have energy, topological charge, and electric charge given respectively by

$$\begin{aligned} E &= \int d^4x \text{Tr} \left(\frac{1}{2} F_{i0} F_{i0} + \frac{1}{4} F_{ij} F_{ij} + \frac{1}{2} D_0 \phi D_0 \phi \right. \\ &\quad \left. + \frac{1}{2} D_i \phi D_i \phi \right), \\ k &= -\frac{1}{16\pi^2} \int d^4x \epsilon_{ijkl} \text{Tr}(F_{ij} F_{kl}), \\ Q_E &= \int d^4x \text{Tr}(D_i \phi F_{i0}) = \int d^4x \text{Tr}(D_i \phi)^2. \end{aligned} \quad (19)$$

We use a Bogomolny argument of the type [23] to give us a bound on the energy, by completing the square

$$E = \int d^4x \text{Tr} \left(\frac{1}{8} \left(F_{ij} \pm \frac{1}{2} \epsilon_{ijkl} F_{kl} \right)^2 + \frac{1}{2} (F_{i0} \pm D_i \phi)^2 + \frac{1}{2} D_i \phi D_i \phi + \frac{1}{8} \epsilon_{ijkl} F_{ij} F_{kl} \mp F_{i0} D_i \phi \right), \quad (20)$$

So we get

$$E \geq 2\pi^2 |k| + |Q_E|, \quad (21)$$

where

$$k = -\frac{1}{16\pi^2} \int d^4x \epsilon_{ijkl} \text{Tr}(F_{ij} F_{kl}),$$

$$Q_E = \int d^4x \text{Tr}(D_i \phi F_{i0}) = \int d^4x \text{Tr}(D_i \phi)^2. \quad (22)$$

The conditions for this bound to be saturated are

$$\begin{aligned} F_{ij} &= \frac{1}{2} \epsilon_{ijkl} F_{kl}, \\ F_{i0} &= D_i \phi, \\ D_0 \phi &= 0. \end{aligned} \quad (23)$$

With the boundary condition on ϕ that it goes to the vacuum expectation value (VEV) $\phi_0 = i\mathbf{q}$ at infinity [5] where \mathbf{q} is an arbitrary imaginary quaternion. The second and third of these are satisfied provided the fields are static and $A_0 = \phi$. Requiring our solutions to obey Gauss' law, $D_i E_i = ig[\phi, D_0 \phi]$, imposes the further equation

$$D^2 \phi = 0. \quad (24)$$

So, to find a dyonic-instanton solution, we can use the ADHM method to calculate a self-dual field strength $F_{\mu\nu}$, then additionally calculate the background scalar field using Eq. (24). An important corollary is the observation that when $\phi = 0$, the solution reduces to precisely that of a pure instanton, and such solutions are in one-to-one correspondence with the pure instanton solutions discussed above.

A. The ADHM construction

To calculate an instanton solution, we use the ADHM construction. We follow an ansatz-based construction outlined in [20]. A good discussion of this can be found in [24].

The main ingredient in the ADHM construction is the ADHM data Δ . This is an $(N + 2k) \times 2k$ matrix, where N is the degree of the gauge group $SU(N)$ or $U(N)$, and k is the instanton number, or topological degree. In the commutative case the entries are usually taken to be real, whereas in the noncommutative case they are taken as

being complex. However, they can be taken to be complex in the commutative case too, with the real solution recovered using the symmetries due to the additional redundancy. Therefore, we will treat the entries as being complex in the remainder of this paper unless otherwise stated. With this in mind, we have

$$\Delta = \begin{bmatrix} \Lambda \\ \Omega \end{bmatrix}, \quad (25)$$

where Λ is an $N \times 2k$ complex matrix and Ω is a $2k \times 2k$ Hermitian matrix. It is often useful for the purpose of performing calculations to treat these as being instead biquaternion-valued matrices (or quaternion-valued, for real matrices). The matrix Ω can always be treated as a $k \times k$ matrix of biquaternions, but Λ is not as straightforward. For some values of N and k there is a similar identification—for example, for the $U(2)$ instantons we consider in this paper, we can always write Λ as a row of N (bi)quaternions. However, in general, this is not possible.

This difficulty is mitigated by the fact that we will always end up considering $\Delta^\dagger \Delta$ in any practical calculation, and as we shall see below, this can always be written in (bi)quaternion form.

The commutative ADHM method involves solving the equation

$$\Delta^\dagger \Delta = \mathbb{1}_2 \otimes f^{-1}, \quad (26)$$

where f is an invertible $k \times k$ matrix, and we can think of $\mathbb{1}_2$ as the quaternion identity. This also means we can look at the ADHM equation above as

$$\text{Im}_{\mathbb{H}}(\Delta^\dagger \Delta)_{ij} = 0, \quad (27)$$

where $\text{Im}_{\mathbb{H}}$ takes the quaternion imaginary part. In the noncommutative case we must modify the ADHM equation (26) to be

$$(\Delta^\dagger \Delta)_{ij} = \mathbb{1}_2 \otimes f_{ij}^{-1} - 4\zeta \sigma_3 \delta_{ij}, \quad (28)$$

which we can view as

$$\text{Im}_{\mathbb{H}}(\Delta^\dagger \Delta)_{ij} = -4\zeta \sigma_3 \delta_{ij}. \quad (29)$$

This solution has some residual freedom—we can transform any solution Δ to

$$\Delta \rightarrow \begin{bmatrix} 1 & 0 \\ 0 & R^T \end{bmatrix} \Delta R \quad (30)$$

to obtain a new solution, where R lies in $O(k)$ if we are using real quaternions, or $SU(k)$ if we are using biquaternions. This additional freedom in the biquaternion case cancels out the additional degrees of freedom from the complexified ADHM parameters. This freedom is also

important in obtaining the moduli space metric (see Appendix C). Once we have solved Eq. (26), or its noncommutative analog, we can use it to calculate the gauge potential and field strength.

To do this, we need to find a zero eigenvector $U(x)$ of Δ^\dagger , normalized so that $U^\dagger U = 1$. There are N such vectors, spanning the nullspace of Δ , satisfying

$$U^\dagger \Delta = \Delta^\dagger U = 0. \quad (31)$$

This implies that U has dimension $N + 2k$ as a complex vector. Once we have this U we can use it to define the gauge potential as

$$A_\mu = U^\dagger \partial_\mu U, \quad (32)$$

and the field strength as

$$F_{\mu\nu} = -4U^\dagger b f \sigma_{mn} b^\dagger U, \quad (33)$$

where b is a $(N + 2k) \times 2k$ matrix whose top $N \times 2k$ part is 0 and whose bottom $2k \times 2k$ part is the identity, and σ_{mn} is as given in (6). This procedure works for both the commutative and the noncommutative cases. An additional subtlety in the noncommutative case comes from the assumption implicit in the above construction that we can factorize the projection operator

$$1 - U\bar{U}, \quad (34)$$

as

$$1 - \mathcal{P} \equiv \delta_{\lambda\kappa} \delta_\alpha^\beta - \mathcal{P}_{\lambda\kappa\alpha}^\beta = \Delta f \bar{\Delta}. \quad (35)$$

This is called the ‘completeness relation’. It is automatically satisfied in the commutative case, however there are some complications in the noncommutative case. The issue is that, whereas the normalization of $U(x)$ is straightforward in the commutative case, there are subtleties in the case where x is itself an operator. We must therefore be careful to pick a good definition for this normalization. These issues were first discussed in [20]. However, this is highly nontrivial as it only affects the value of U and not the validity of the remainder of the solution—it is only necessary if one is constructing an explicit expression for the gauge potential, which we are not. The only point we use U is in Appendix D, and there we take it in the limit $x \rightarrow \infty$ in which any noncommutative effects (which go as $\frac{\tilde{\kappa}}{x^r}$ for some positive integer r) are automatically neglected. This does not affect our results though a full investigation might be a fruitful topic for future research.

B. The moduli space

The moduli space of instanton solutions is the space of inequivalent solutions to the self-dual Yang-Mills

equations (26). This was first introduced for instantons in [11]. Calculating the dynamics of an individual instanton solution over a period of time is difficult. However, for sufficiently slow velocities we can approximate such a solution by a slow transition between different instanton solutions with marginally different initial conditions. This corresponds to motion on the moduli space. For a review of techniques and applications see e.g., [6,12,13,25]. The moduli space is parametrized by the $4kN - 4$ free ADHM parameters, which are called the collective coordinates. To define small velocities, we must introduce a moduli space metric. To do this we look at small fluctuations $A_m(x) + \delta A_m(x)$. If this is also to be a solution to the equations (and hence lie in the moduli space), the δA_m must satisfy the linearized self-duality equation

$$\mathcal{D}_m \delta A_n - \mathcal{D}_n \delta A_m = \epsilon_{mnl} \mathcal{D}_l \delta A_l. \quad (36)$$

In addition, it must not be related to $A_n(x)$ by a local gauge transformation. We therefore require the solutions to be orthogonal to gauge transformations. To define this orthogonality, we take the natural metric on the space of all solutions

$$g(\delta A_m(x), \delta A'_m(x)) = \int d^4x \text{Tr}(\delta A_m(x) \delta A'_m(x)), \quad (37)$$

and then use this to induce a metric on the moduli space after quotienting out the gauge-equivalent solutions. We then require that under this metric, zero modes $\delta A_i(x)$ are orthogonal to all gauge transformations $D_i \Lambda$. This is equivalent to satisfying

$$D_i \delta A_i = 0. \quad (38)$$

For small perturbations, we get the following action on the moduli space [12,26]

$$S = \frac{1}{2} \int d^5x \text{Tr}(F_{i0} F_{i0} - D_i \phi D_i \phi + D_0 \phi D_0 \phi). \quad (39)$$

If we neglect terms of order $z^2 |q|^2$, where $z(t)$ refers to any of the collective coordinates on the moduli space, we get the effective action

$$S = \frac{1}{2} \int dt (g_{rs} \dot{y}^r \dot{y}^s - |q|^2 g_{rs} K^r K^s), \quad (40)$$

where the K_r are Killing vectors of the moduli space and satisfy $D_m \phi = |q| K^r \delta_r A_m$. Then Eq. (40) is the sum of a free instanton and the potential

$$V = \frac{1}{2} \int d^5x \text{Tr}(D_i \phi D_i \phi) = \frac{|q|^2}{2} \int dt g_{rs} K^r K^s. \quad (41)$$

This solution is valid in the limit

$$\dot{z}^2, \quad |q| \leq 1, \quad (42)$$

where we can ignore terms of order $\dot{z}^2|q|^2$ and higher. The geometric interpretation of this is both that the kinetic energy of the instanton solution is sufficiently small, and that the potential evaluated on the instanton solutions, which lie on the moduli space, is shallow compared to the potential on non-BPS solutions evaluated off the moduli space. This allows us to imagine our approximate solution as lying in a steep valley given by the locally small potential around the moduli space solutions, where the small kinetic energy prevents our dynamics from, ‘climbing away’ from the moduli space.

C. The complex subspace

There is one final technical point to discuss, which applies to both pure and dyonic instantons. The moduli space has several subspaces, which are preserved under the geodesic motion. This means a geodesic beginning in one of these subspaces (i.e., whose initial tangent vector lies in that subspace) will remain in it throughout its motion.

The subspace we are interested in is as follows. The moduli space is a manifold over the collective coordinates \mathbf{z} . However, as we saw in Sec. III A these collective coordinates are elements of the ADHM matrix Δ and therefore are parametrized by the (bi)quaternions. That algebra can be thought of as $\mathbb{C} \times \mathbb{C} \times \mathbb{H}$. Therefore, in the same way that the quaternions contain an invariant complex subspace \mathbb{C} , the biquaternions have the subspace $\mathbb{C} \times \mathbb{C}$. We can therefore restrict from the full moduli space where the collective coordinates are biquaternions, to a submanifold where they lie in $\mathbb{C} \times \mathbb{C}$.

This corresponds to conjugating all the moduli space coordinates by a unit quaternion q , e.g., $\tau \rightarrow q\tau\bar{q}$. This corresponds geometrically to leaving the real quaternion part fixed, whilst the imaginary quaternion is rotated around an axis in S^3 represented by q . Imposing invariance under such rotations corresponds to requiring our solutions to be fixed points under this rotation, which constrains them to lie in a two-dimensional plane within the four dimensional quaternions. Because $\bar{q}q = 1$, if we multiply two (bi)quaternions together and apply this rotation to each of them then the result is that the entire product is rotated—e.g.,

$$\Delta^\dagger \Delta \rightarrow q\Delta^\dagger \bar{q}q\Delta\bar{q} = q\Delta^\dagger \Delta\bar{q}. \quad (43)$$

We can therefore think of all our equations and objects (for example the scalar field and potential) as being rotated in the same overall way. In the commutative space, for pure instantons we can see the invariance of this subspace automatically, since the elements of $\mathbb{C} \in \mathbb{H}$ automatically commute with all other elements, meaning that they form an ideal within that group (and ideals are invariant subspaces) [27]. For dyonic instantons, we must choose the

imaginary direction to be the same as the VEV in $SU(2)$, since otherwise the VEV will not be preserved. The result is that the transformation maps solutions to solutions, and so the fixed point manifold thus generated is also a geodesic submanifold of our moduli space. In the noncommutative case, the presence of the noncommutative parameter means that the spacetime coordinates do not automatically commute. The only complex subspace which is preserved in this case is the complex subspace spanned by $\{1, \sigma_3\}$, as, since σ_3 is the direction associated with the noncommutativity, it is preserved under rotations of the space, and 1 commutes with everything. We must then align the plane within \mathbb{H} that we are preserving with this direction. Hence we see, as would be expected, the presence of a noncommutative parameter reduces the symmetries of the theory.

Calculations on the full quaternion moduli space are very computationally expensive, and this subspace is often much easier to run simulations on. In addition, the fact that elements in this subspace commute makes solving the ADHM equations on this restricted part of the theory much easier.

IV. THE TWO INSTANTON SOLUTION

Now we have discussed the technical background, we present our work on the dynamics of the noncommutative $U(2)$ 2-instanton. First, we review the single $U(2)$ instanton as presented in [18]. This is necessary to test the two-instanton solution in the appropriate limits. Next we derive the ADHM equations for the two-instanton case, using biquaternion coordinates. We were unable to find a solution for the full moduli space; however, we were able to find a solution for the geodesic submanifold discussed in Sec. III C. This corrects the solution in [14].

After finding this solution we use it to derive the metric and potential for the relevant moduli space, and show that the metric and potential behave suitably in the commutative limit and in the limit of the instantons being far separated.

A. The single $U(2)$ instanton

First, we state the solution for a single $U(2)$ instanton in noncommutative space. We will follow [18]; however, we rederive their solution in our notation. One key difference is that the relation between their ζ' and our ζ is $\zeta' = 2\zeta$. Other discussions of the solution can be found in [20,19]. First, for the single noncommutative $U(2)$ instanton, the ADHM data has the form

$$\begin{bmatrix} v_R + v_I \sigma_3 \\ X - x' \end{bmatrix}; \quad v_R, v_I, X, x' \in \mathbb{H}. \quad (44)$$

As discussed in [18], we can set $X - x' = 0$ by a symmetry transformation related to the centre of mass. Then we can solve for v_I in terms of the free parameter v_R .

$$v_I = -\frac{2\zeta v_R}{|v_R|^2}; \quad v_R \in \mathbb{H}. \quad (45)$$

This gives us four ADHM coordinates, as required. Now we have this, we can calculate the metric and potential using the method discussed in Appendixes B and D. The potential is equal to

$$\mathcal{V} = 8\pi^2 |\mathbf{q}|^2 \left(\rho^2 - \frac{16\zeta^2}{\rho^2} \cos^2(\theta) \right), \quad (46)$$

and the metric is

$$ds^2 = 8\pi^2 \left(dv_R^2 + dv_I^2 - \frac{(v_R dv_I - \bar{v}_I dv_R)^2}{|v_R|^2 + |v_I|^2} \right). \quad (47)$$

Here $|\mathbf{q}|$ is the VEV of the scalar field ϕ , $v_R = \rho \cos(\theta)$ and $v_I = \rho \sin(\theta)$.

B. Two U(2) instantons

We now move on to the case of two U(2) instantons. In the commutative case, a solution was found for the real quaternions [and with gauge group SU(2)] in [13]. A solution for the noncommutative case was postulated in [14]; however, this is not in fact correct, and an alternative solution is therefore presented here. We were unable to find a solution for the full moduli space, but we obtained a solution for the subspace defined in Sec. III C. For the case of two U(2) instantons, the ADHM data has the form

$$\Delta = a - bx; \quad a = \begin{bmatrix} \Lambda \\ \Omega \end{bmatrix} = \begin{bmatrix} v & w \\ \tau & \sigma^* \\ \sigma & -\tau \end{bmatrix}, \quad b = \begin{bmatrix} 0 & 0 \\ 1 & 0 \\ 0 & 1 \end{bmatrix}. \quad (48)$$

Note that here Ω is constrained to be Hermitian (under complex conjugation) rather than symmetric, as in the real ADHM construction. v , w , and σ lie in the biquaternions; however, due to the requirement that Ω be hermitian, τ remains a member of \mathbb{H} . Proceeding as in Sec. III A, Eq. (26) gives the following. First, the diagonal equations

$$\begin{aligned} v^\dagger v + |\tau|^2 + \sigma^\dagger \sigma &= f_{11}^{-1} \mathbb{1} + 2\zeta \sigma_3, \\ w^\dagger w + |\tau|^2 + (\sigma^\dagger \sigma)^* &= f_{11}^{-1} \mathbb{1} - 2\zeta \sigma_3. \end{aligned} \quad (49)$$

Next, the off-diagonal constraints are given by

$$\begin{aligned} v^\dagger w + \bar{\tau} \sigma^* - \sigma^\dagger \tau &= f_{12}^{-1} \mathbb{1}, \\ w^\dagger v + (\sigma^\dagger)^* \tau - \bar{\tau} \sigma &= f_{12}^{-1} \mathbb{1}. \end{aligned} \quad (50)$$

This gives a total of four equations for the complex ADHM constraints. For completeness we list them here

$$\begin{aligned} 2\text{Im}_{\mathbb{H}}(\bar{\sigma}_R \sigma_I) - \text{Im}_{\mathbb{H}}(\bar{w}_R w_I) + \text{Im}_{\mathbb{H}}(\bar{v}_R v_I) &= 0, \\ \text{Im}_{\mathbb{H}}(\bar{w}_R w_I) + \text{Im}_{\mathbb{H}}(\bar{v}_R v_I) &= -4\zeta \sigma_3, \\ \text{Im}_{\mathbb{H}}(\bar{\tau} \sigma_I) &= \frac{\text{Im}_{\mathbb{H}}(\bar{w}_R v_I + \bar{v}_R w_I)}{2} \equiv \frac{\Upsilon}{2}, \\ \text{Im}_{\mathbb{H}}(\bar{\tau} \sigma_R) &= \frac{\text{Im}_{\mathbb{H}}(\bar{w}_R v_R + \bar{v}_R v_I)}{2} \equiv \frac{\Lambda}{2}. \end{aligned} \quad (51)$$

As a check, if we assume that our solutions to the ADHM equations are entirely real and that $\zeta = 0$, we have the complex imaginary parts of all our variables being 0, and we have only the one equation which is not trivially satisfied (just as in [13])

$$\text{Im}_{\mathbb{H}}(\bar{\tau} \sigma_R) = \frac{\text{Im}_{\mathbb{H}}(\bar{w}_R v_R)}{2}. \quad (52)$$

It should be noted that no new degrees of freedom are introduced compared to the real ADHM equations. Complexifying v , w , and σ adds twelve degrees of freedom. However, each of the three new equations affecting the imaginary part of an expression adds three constraints, giving a total of nine. Recall that we have a residual O(2) symmetry on our solutions to the ADHM equation in the quaternion case, which is promoted to a U(2) symmetry in the biquaternion case allows us to remove a further three degrees of freedom. This gives a total of 12 degrees of freedom removed, canceling the number of new parameters and showing that there are no new solutions. We have checked this explicitly by constructing the transformation taking a commutative ADHM solution with biquaternion coordinates to the standard solution parametrized by quaternions. However, this is time consuming and not especially illuminating.

We were unable to solve these equations for the full biquaternion valued space, but we were able to calculate solutions restricted to the complex subspace defined in Sec. III C. After some calculation (see Appendix A), we get

$$\begin{aligned} v_I &= \frac{-2\zeta v_R \sigma_3}{|v_R|^2}, \\ w_I &= \frac{-2\zeta w_R \sigma_3}{|w_R|^2}, \\ \sigma_R &= \frac{\tau \text{Im}(\bar{w}_R v_R + \bar{v}_R w_I)}{2|\tau|^2} \\ &= \frac{(|v_R|^2 |w_R|^2 + 4\zeta^2)}{2|\tau|^2 |v_R|^2 |w_R|^2} \tau \text{Im}_{\mathbb{C}}(\bar{w}_R v_R) \sigma_3, \\ \sigma_I &= \frac{\tau \text{Im}_{\mathbb{C}}(\bar{w}_R v_I + \bar{v}_R w_I)}{2|\tau|^2} \\ &= -\frac{\zeta(|w_R|^2 + |v_R|^2)}{|\tau|^2 |v_R|^2 |w_R|^2} \tau \text{Im}_{\mathbb{C}}(\bar{w}_R v_R \sigma_3) \sigma_3. \end{aligned} \quad (53)$$

We can check our assumption about the symmetries by checking both that our solution really does solve the ADHM equations, and that there are no residual symmetries remaining. To show there are no residual symmetries, we consider a general U(2) transformation

$$\begin{bmatrix} v & w \\ \tau & \sigma^* \\ \sigma & -\tau \end{bmatrix} \mapsto \begin{bmatrix} v' & w' \\ \tau' & \sigma'^* \\ \sigma' & -\tau' \end{bmatrix} = \begin{bmatrix} av - \bar{b}w & bv + \bar{a}w \\ (|a|^2 - |b|^2)\tau - ab\sigma - \bar{a}\bar{b}\sigma^* & 2\bar{a}b\tau - b^2\sigma + \bar{a}^2\sigma^* \\ 2\bar{a}\bar{b}\tau + a^2\sigma - \bar{b}^2\sigma^* & -(|a|^2 - |b|^2)\tau + ab\sigma + \bar{a}\bar{b}\sigma^* \end{bmatrix}. \quad (55)$$

Now, in Appendix A we use the residual symmetry to do two things. First, we require that $\text{Re}_{\mathbb{C}}(\bar{\tau}\sigma) = 0$. This imposes the condition that σ has no component proportional to τ . Second, we require that $\bar{w}_R w_I = \bar{v}_R v_I$. We need to work out the form of the transformation in Eq. (55) so that the new variables v' , τ' etc., also satisfy these conditions. If the form of the transformation is completely determined by this, then we know we have no remaining symmetries to consider.

To aid in this, we write

$$\begin{aligned} a &= \cos\chi(\cos\theta + i\sin\theta), \\ b &= \sin\chi(\cos\phi + i\sin\phi). \end{aligned} \quad (56)$$

The first of these conditions, $\text{Re}_{\mathbb{C}}(\bar{\tau}'\sigma') = 0$ requires that $|a|^2 - |b|^2 = 0$, and hence that both $\chi = \frac{n\pi}{4}$ for n from 1 to 7, and also $\theta = -\phi$. This condition on χ gives the dihedral group of order 16 as a group of discrete rotations. The implications of this are discussed in [13]. Now, we look at the second part of our symmetry, which is unique to the noncommutative case. Keeping $\bar{w}'_R w'_I = -\bar{v}'_R v'_I$ requires $\cos(2\theta) + i\sin(2\theta) = 0$. This leads to

$$\theta = \frac{n\pi}{2}; \quad \text{e.g.,} \quad \theta = 0, \frac{\pi}{2}, \pi, \frac{3\pi}{2}, \dots \quad (57)$$

Now, $\theta = \frac{n\pi}{2}$ multiplies a , b by ± 1 and so does not change the symmetries in [13]. If we set $\theta = 0, \pi$ we multiply a and b by $\pm i$ and $\mp i$, respectively. This does not change τ , but sends $\sigma \rightarrow -\sigma$. It also interchanges the complex real and imaginary parts of v' and w' . Between them these two conditions fully fix the form of the transformation in Eq. (55) and therefore there is no residual symmetry.

The next step is to calculate the scalar field, potential, and metric. The calculations and results are long and not particularly illuminating, and so are given in Appendixes B and C. Now we will go on to investigate the dynamics on the moduli space via numerical methods.

V. TWO-INSTANTON DYNAMICS

In this section we discuss the dynamics of the instantons on the noncommutative two instanton moduli space we

$$\Delta \mapsto \begin{bmatrix} 1 & 0 \\ 0 & R^\dagger \end{bmatrix} \Delta R; \quad R = \begin{bmatrix} a & b \\ -\bar{b} & \bar{a} \end{bmatrix};$$

$$a, b \in \mathbb{C}, \quad |a|^2 + |b|^2 = 1. \quad (54)$$

This generates the transformation

have constructed, solving for motion on the moduli space numerically. Where possible we use the same numerical algorithms developed in [13] to produce the following figures, and for when the scattering problem becomes more complex we used a new numerical algorithm.

A. The setup

The ADHM data are in terms of $v = v_R + iv_I, w_R + iw_I, \sigma = \sigma_R + i\sigma_I$ and τ . We showed in Appendix A that v_I, w_I and σ depend on the collective coordinates v_R, w_R , and τ . As stated in Sec. III C, we are working on the subspace of the total moduli space with the collective coordinates in $\mathbb{C} \times \mathbb{C}$ rather than $\mathbb{C} \times \mathbb{H}$. This means that v and w are in $\mathbb{C} \times \mathbb{C}$, whilst τ is in \mathbb{C} (since it lies on the diagonal, and Δ is Hermitian with respect to the complex structure). As is standard [23], we interpret v, w as describing the embedding of the instantons into the gauge group, with $\tilde{\rho}_1 = |v|$ and $\tilde{\rho}_2 = |w|$ giving the physical size and τ giving the position. This is shown in Fig. 1. We also

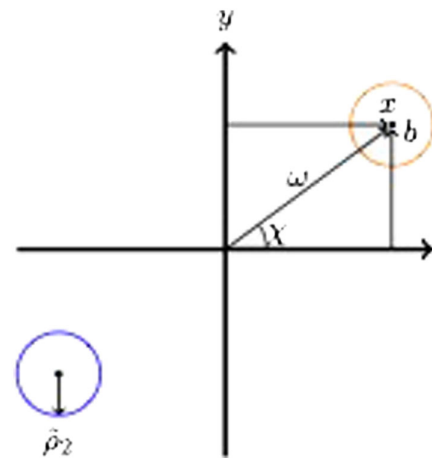


FIG. 1. The setup of the instantons. The instantons are located at $\pm(x, b) = (\omega \cos(\chi), \omega \sin(\chi))$. They have size $\tilde{\rho}_i = \sqrt{\rho_i^2 + \frac{4\zeta^2}{\rho_i^2}}$.

rewrite our independent ADHM coordinates in polar form as

$$\begin{aligned} v_R &= \rho_1(\cos(\theta_1) + i \sin(\theta_1)), \\ w_R &= \rho_2(\cos(\theta_2) + i \sin(\theta_2)), \\ \tau &= \omega(\cos(\chi) + i \sin(\chi)). \end{aligned} \quad (58)$$

It is convenient to describe the initial conditions in cartesian coordinates b and x as indicated in Fig. 1. The relation between the parameters b , x and ω , χ is

$$\begin{aligned} x &= \omega \cos(\chi), \\ b &= \omega \sin(\chi), \\ \omega &= \sqrt{b^2 + x^2}, \\ \chi &= \arctan(b/x). \end{aligned} \quad (59)$$

Now, using the equations

$$\begin{aligned} v_I &= \frac{-2\zeta v_R \sigma_3}{|v_R|^2}, \\ w_I &= \frac{-2\zeta w_R \sigma_3}{|w_R|^2}. \end{aligned} \quad (60)$$

It follows that in the noncommutative case, the total instanton size ρ_i is defined as

$$\tilde{\rho}_i = \sqrt{\rho_i^2 + \frac{4\zeta}{\rho_i^2}}, \quad (61)$$

where the index i in ρ_i is either 1 or 2, referring to the magnitude of v or w respectively. Calculating the scattering with general ρ_1 and ρ_2 , and with general gauge embedding is very computationally expensive for the noncommutative case. Therefore, we did a lot of the simulations in the ‘orthogonal’ case where $\rho_1 = \rho_2$ and the relative gauge angle between the two instantons is $\theta_1 - \theta_2 = \pi/2$. There are several technical issues which emerged. First of all, at the collision point there are two ingoing and two outgoing paths where the instanton positions nearly coincide; it is difficult to work out which ingoing and outgoing paths ought to be connected. The plotting program we used appears to choose sensibly except in a few cases where it appears to connect the wrong pairs, as evidenced by a discontinuity in the path near the origin. This can be seen on several of the graphs, e.g., in Fig. 6.

The second issue is with the parametrization of the instanton position in terms of τ . The position of the instanton is given by the eigenvalues of the submatrix

$$\begin{bmatrix} \tau & \sigma^* \\ \sigma & -\tau \end{bmatrix} \quad (62)$$

of the ADHM data [13]. Recall that

$$\begin{aligned} \sigma_R &= \frac{\text{Im}(\bar{w}_R v_R + \bar{w}_I v_I)}{2} = \frac{(|v_R|^2 |w_R|^2 + 4\zeta^2)}{2|\tau|^2 |v_R|^2 |w_R|^2} \tau \text{Im}(\bar{w}_R v_R), \\ \sigma_I &= \frac{\text{Im}(\bar{w}_R v_I + \bar{w}_I w_I)}{2} = -\frac{\zeta(|w_R|^2 + |v_R|^2)}{|\tau|^2 |v_R|^2 |w_R|^2} \tau \text{Im}(\bar{w}_R v_R \sigma_3). \end{aligned} \quad (63)$$

In the subspace under discussion, and in the coordinates we are using, this becomes

$$\begin{aligned} \sigma_R &= \frac{i(\rho_1^2 \rho_2^2 + 4\zeta^2)(\cos(\chi) + i \sin(\chi)) \sin(\theta_1 - \theta_2)}{2\rho_1 \rho_2 \omega}, \\ \sigma_I &= \frac{-i\zeta(\rho_1^2 + \rho_2^2)(\cos(\chi) + i \sin(\chi)) \cos(\theta_1 - \theta_2)}{\rho_1 \rho_2 \omega}, \end{aligned} \quad (64)$$

At large τ , the matrix is effectively diagonal, and so the positions of the two instantons can be approximated by τ and $-\tau$ respectively. At small values of τ , however, σ becomes very large and therefore $\pm\tau$ is no longer a good description. A better approach is to diagonalize the full matrix which gives the parametrization $\pm\sqrt{\tau^2 + \sigma^2}$ for the position (note that this is in general a complex number), though this can give a discontinuity at the origin due to the presence of the square root, with both positive and negative values. In the commutative case this is the true position of the instanton. In the noncommutative case, the noncommutativity of the underlying space means that the meaning of, ‘true position’ is not clear; however, it still makes more sense to use the $\sqrt{\tau^2 + \sigma^2}$ parametrization, as the presence of ζ in σ means that this becomes more important (as shown in Fig. 2). We now move on to looking at the graphs.

B. Pure instantons

We start with the four-parameter orthogonal instantons. There are two procedures we can use to investigate the moduli space dynamics when noncommutativity is introduced. The first is to start off with a particular example of commutative scattering and see how turning on the noncommutativity affects this. The second relies on the fact that choosing a value for the noncommutative parameter ζ sets an overall scale. We can therefore ‘scan’ the parameter space for interesting behavior by varying one of the other parameters at a time for a fixed value of ζ . It should be noted that this scanning process is not in itself sensitive to periodic ambiguities in the scattering angles—e.g., instantons moving parallel and not interacting and instantons reflecting directly off each other would both register a scattering angle of zero. Therefore we must supplement this scanning by looking at individual plots to check the interpretation of the scattering angles we have found.

Both these methods have their uses and we will use each in turn. With the first method, we will see how a typical

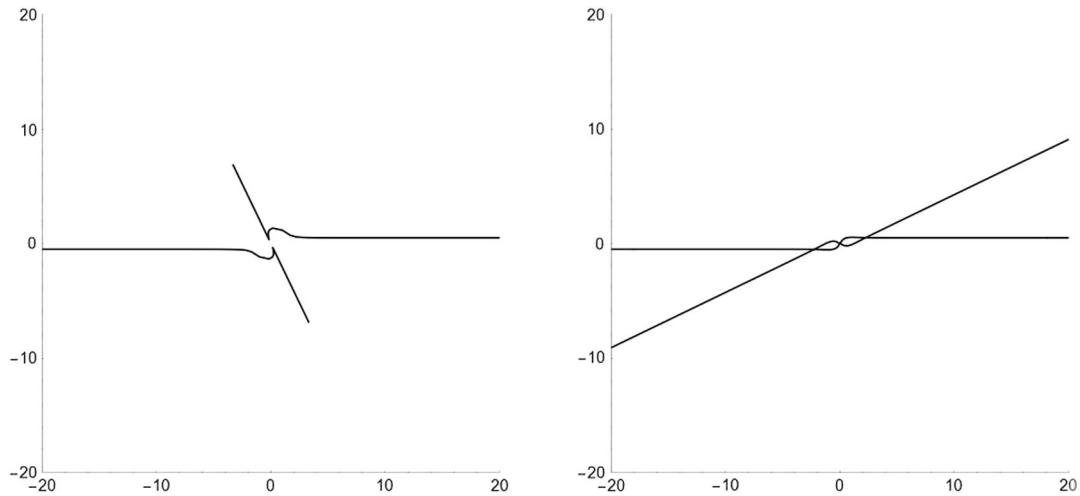


FIG. 2. Scattering of dyonic instantons with $b = 0.5$ and $\zeta = 1.15$. Both plots are solutions of the same initial set up, with different choices of parametrization of the position. The left plot shows the $|\tau|$ parametrization, the right shows $\pm\sqrt{\tau^2 + \sigma^2}$. The radii of the instantons are not shown. In this case the σ behavior dominates and after the interaction the position of the instantons goes as $\frac{1}{|\tau|}$. Note that after 2,400 time steps the $\sqrt{\tau^2 + \sigma^2}$ had left the plot region, whereas the τ case has been run for 50,000 time steps and still has not left the plotted area. This is because the size of the instantons (hence v and w) becomes very large and so σ dominates τ in the definition of the instanton position, so that merely plotting τ is a very inaccurate approximation to the position.

example of scattering changes with the parameter ζ . We will also investigate what happens to the orthogonal scattering in the noncommutative case. We will then use the second method to see if there is interesting systematic behavior associated with the other ADHM parameters.

First, we take a typical example of scattering in the commutative case, and see what happens when we add in noncommutativity. In this case, the parameters $\{\rho, \theta, b, x\}$ take the values $\{1, 0, 0.5, 50\}$ and their initial derivatives are $\{0, 0, 0, -0.03\}$. The change in scattering angle as we change the value of ζ from 0 to 5 is shown in Fig. 4. The most obvious feature is the presence of a peak. This is a general feature of scattering as we change ζ —see Fig. 3. The peak is hard to resolve numerically—there seems to be a discontinuity. To analyze this we can zoom in on that

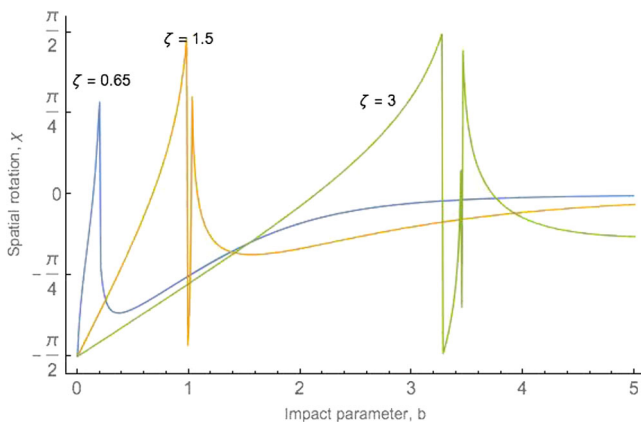


FIG. 3. Plot of scattering angle vs impact parameter for different values of ζ . From left to right we have $\zeta = \{0.65, 1.5, 3\}$.

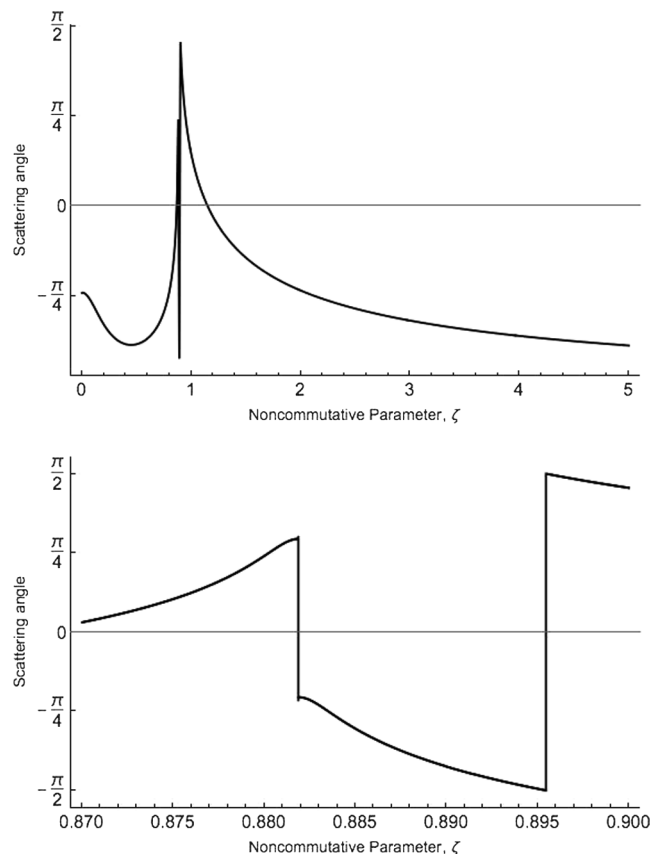


FIG. 4. Change of scattering angle (above) with noncommutative parameter ζ for $b = 0.5$, with the other parameters as discussed in the main body of the text. On the below graph is shown the area around the discontinuity, which seems to be a region where the numerics have confused $\pm\theta$.

section of the graph (Fig. 6). Part of the issue seems to be a numerical error based on the code jumping between $\pm\theta$ at $\pi/4$ and $\pi/2$. This cannot completely explain the phenomenon however. Looking at the graphs in Fig. 6, the instantons appear to merge then divide again in a way that, ‘swaps over’ the ingoing and outgoing tracks. This may indicate the presence of a bound state at the cusp, which the numerics cannot fully resolve. Another possibility is that there is suddenly a second scattering at right angles. It is not clear why there should be such a sharp transition, but perhaps it happens when the instantons become large enough to overlap during the scattering process. This would be a good topic for future work with more powerful numerical methods.

In general, the effect of the noncommutativity is to increase the repulsion between the instantons. Initially, the instanton scattering angle seems to rotate anticlockwise, going from glancing off each other, to moving parallel,

to crossing over. This occurs rapidly as ζ changes from 0.85 until about 0.88 (Fig. 5).

At the first apparent discontinuity, the instantons change from moving across each others paths, to repelling and turning back on themselves, so that their paths form a loop near the interaction point. This change happens somewhere between $\zeta = 0.8818695$ and $\zeta = 0.88187$. The beginnings of the looping behavior can be seen in the first graph in Fig. 6, however as can be seen in the second graph there is no way of assigning the trajectories to different instantons. This is a general feature of instanton dynamics—you cannot distinctly separate instantons when they get too close [23].

Some of the issue with correctly defining the angle can be seen from the bottom two graphs in Fig. 6, where the loops are joined in two different ways. Comparing the last graph in 6, the last graph in Fig. 4 and the first graph in Fig. 7 indicates that the particles seem to loop back on

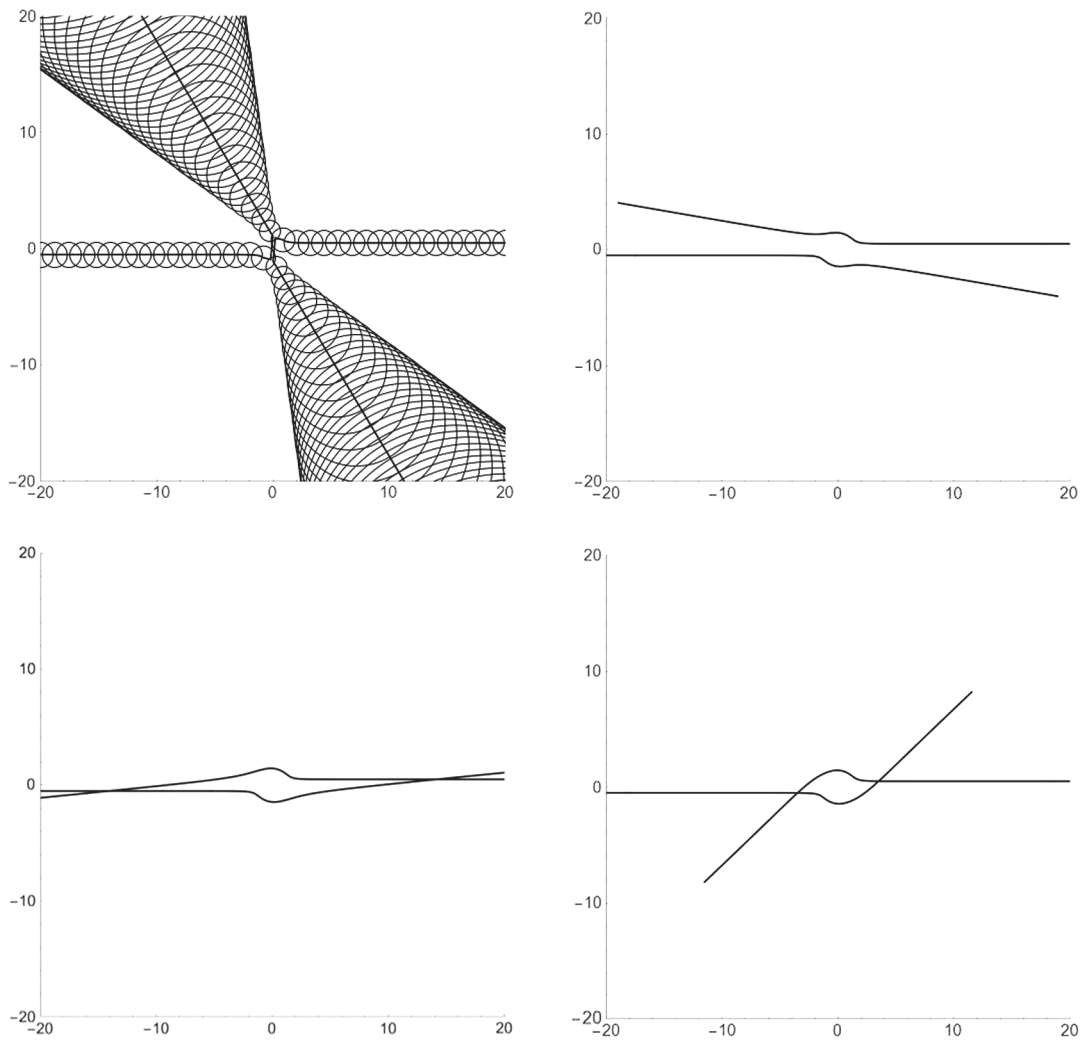


FIG. 5. Scattering for two instantons with $b = 0.5$, and, moving in each row from left to right, $\zeta = \{0.1, 0.86, 0.87, 0.88\}$. This corresponds to the region to the left of and around the peak in Fig. 4 where the sizes are not shown this is in order to make the trajectories clearer. Note that the instantons go from glancing off one another, to moving parallel, to crossing over, and then deflecting.

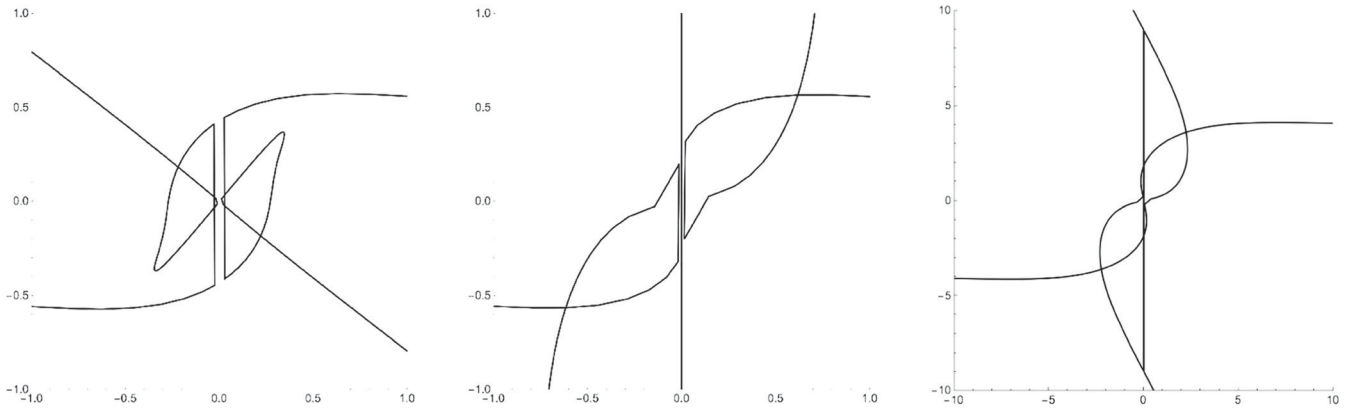


FIG. 6. Graphs of the interaction around the peak, zoomed in at the center, with $\zeta = \{0.8187, 0.89, 0.9\}$. The vertical lines on the graph are the results of confusion about which parts of the trajectory belong to which instanton, and can be ignored. A more detailed interpretation of the graphs is given in the main text.

themselves. This is further evidence for the fact that discontinuities in the scattering angle graph 6 are based on a breakdown of the notion of the instanton positions as they begin to intersect.

After the peak (Fig. 7), the scattering angle appears to rotate clockwise—the loop at the interaction point is, ‘unwound’. This leads to them then repelling entirely before the angle widens to about $\pi/4$, with the instantons repelling rather than glancing off each other as they did at the start.

We observed this behavior for a number of different setups, including where the instantons began too far apart to originally interact. An overall feature of all this graphs is that whereas in the commutative case the instantons shrink through zero size then expand again, in the noncommutative case, as we would expect, they shrink to a finite size before expanding since due to the noncommutativity the zero size point cannot be reached.

Plotting the scattering angle for differing values of the impact parameter b shows the same distinctive spike for a particular value of b (Fig. 3). As a numerical check, if we interchange the roles of b and ζ by plotting the scattering angle for varying ζ whilst keeping b fixed, the spike appears at the same (b, ζ) coordinates. If we plot the graphs of scattering angle vs impact parameter for different values of ζ we see that the overall behavior stays the same, however the position of the peak moves to the right as ζ increases as shown in Fig. 3. This behavior only appears when $\zeta \neq 0$, and therefore seems to be unique to the noncommutative case. This would be another topic for further investigation.

The next case we will look at is the case where the scattering is orthogonal in the commutative case (so $b = 0$). This remains consistently orthogonal in the noncommutative case—see Fig. 8. Overall the scattering keeps its perpendicular character. We can explain this analytically in a similar way as in the commutative case in [13]. As discussed above, the location of the instantons is described

by a combination of τ and σ . Because σ behaves like $1/|\tau|$, the change in which parameter dominates happens when $|\tau| = |\sigma|$. Recall the definitions of τ and σ in Eq. (64). For the case of orthogonal scattering, $\chi = 0$. Therefore $\tau = \omega$, and so lies entirely on the x -axis. On the contrary, σ is proportional to i and so lies on the y -axis. Therefore, as the dominant parameter in the position changes between τ and σ , the instanton motion changes from the x -axis to the y -axis and so they scatter orthogonally.

We then used the scanning method to look for interesting behavior amongst the other parameters. Fixing ζ fixes the length scale of the system, therefore we investigated the behavior of the system keeping ζ at a constant value of 1, and looking at how the scattering angle of the instantons depends on the other parameters. The variables for which there was notable behavior were $\dot{\rho}$ and $\dot{\theta}$. These showed similarly interesting behavior in both cases, and so we will discuss them together. As can be seen in Fig. 9, in both cases, a small perturbation in $\dot{\rho}$ and $\dot{\theta}$ causes almost orthogonal scattering, no matter what the initial scattering angle. The difference is that there seems to be jump of the scattering angle from positive to negative, for positive and negative $\dot{\theta}$, which is not present for $\dot{\rho}$. However, it is unclear even from individual scattering graphs if this is a misidentification of incoming and outgoing particles. Even if there is no scattering in the, ‘base’ case where both are zero, as in Fig. 8, we still get the same orthogonal scattering behavior; however, there is not the same jump in scattering angle at the origin. The reason for this behavior seems to be that changing either of these parameters from zero makes the instanton size very large, causing a high degree of interaction (and hence orthogonal scattering) no matter what the initial separation is. There is a subtlety in that $\dot{\rho}$ is not the variation in the actual size, but only in the parameter ρ . The variation in the actual size is given by

$$\dot{\rho} = \frac{\dot{\rho}\rho - \frac{4\zeta^2\dot{\rho}}{\rho^3}}{\sqrt{\rho^2 + \frac{4\zeta^2}{\rho^2}}}. \quad (65)$$

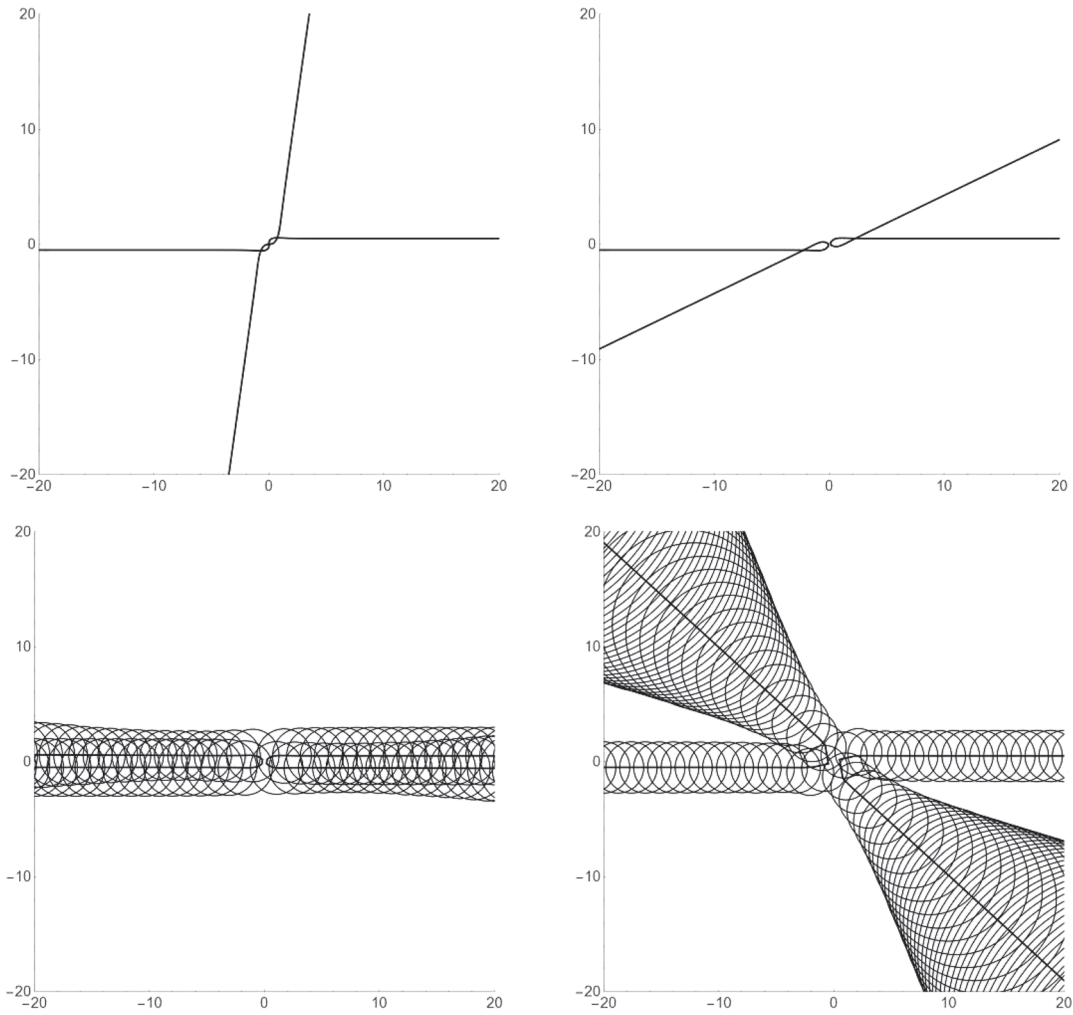


FIG. 7. Scattering for two instantons with $b = 0.5$ and $\zeta = 0.9, 1, 1.15, 2$. This corresponds to the right side of the peak. Note that the instanton angle begins to turn back on itself, until the scattering becomes a direct repulsion $\zeta = 1.15$, then opens to about $\pi/4$.

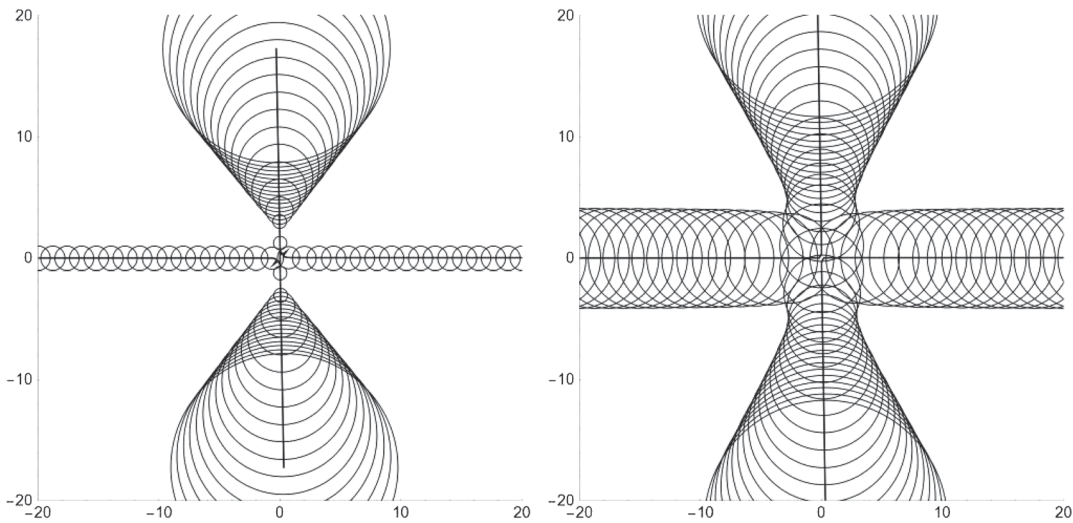


FIG. 8. Examples of scattering behavior for the orthogonal scattering with $b = 0$ for $\zeta = \{0, 2\}$.

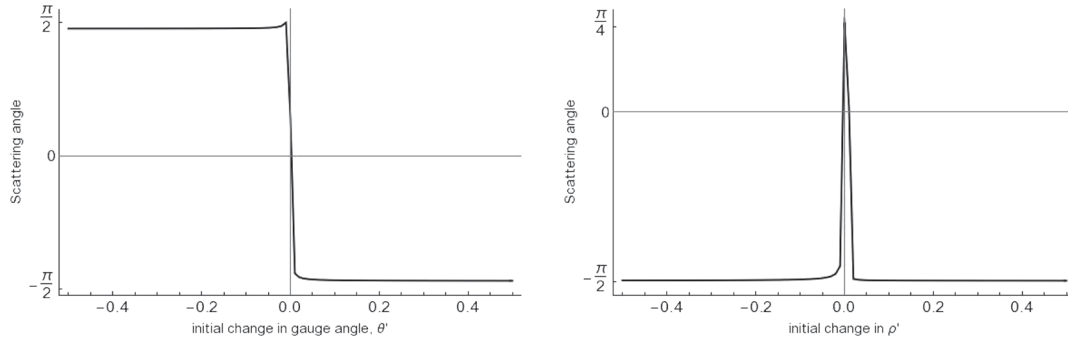


FIG. 9. (left) Graph showing variation of scattering angle vs starting velocity gauge angle $\dot{\theta}$ for $b = 0.5$ and $\zeta = 1$. Note the jump in scattering angle between positive and negative $\dot{\theta}$. (right) Graph showing variation of scattering angle vs $\dot{\rho}$ for $b = 0.5$ and $\zeta = 0.1$. Note that here there is no jump in the scattering angle, unlike in the case of $\dot{\theta}$.

Therefore, $\dot{\rho}$ is a good approximation when $2\zeta/\rho$ is small. We have been careful to only consider such cases. We now move on to dyonic instantons. We follow the same method as before. First we look at how changing ζ changes a specific case of scattering. Then we use the scanning technique to look for interesting behavior linked to varying the ADHM parameters. In the dyonic case, the length scale is still set by ζ , however the scale of the time dimension is no longer arbitrary, but is set by $|q|$. Therefore, we must consider the consequences of varying both.

Looking at specific scattering examples, we again see that the noncommutative parameter initially introduces a repulsive effect (e.g., Fig. 10). Here, the basic values of the parameters are as in the pure case, except that we give θ a small initial velocity of 0.1 in order to avoid numerical issues. Any changes to these parameters will be discussed in the captions to the graphs. As discussed in [13], dyonic instantons oscillate along their motion, and this effect is much more observable with the noncommutativity

turned on. Scanning along the scattering angle in both the commutative and noncommutative case gave very noisy graphs from which it is hard to deduce any global behavior. However we found some interesting examples of orbiting behavior, especially for small q relative to the other parameters—a particularly impressive example is Fig. 11.

We can then systematically look for interesting behavior amongst the remaining parameters. A recurring feature was the presence of stable combinations of ζ and q for which there was a clear pattern of behavior with no observable pattern outside of these regions.

We started by looking at varying θ , but this did not yield any interesting systematic behavior—only random noise. We then looked at ρ —here there seemed to be a window where the behavior matched the commutative case, e.g., with $\zeta = 0.1$ and $q = 0.1$, as shown in Fig. 12. Exploring around that point showed that the behavior persisted with roughly $\zeta < 1$ and with $q > 0.08$.

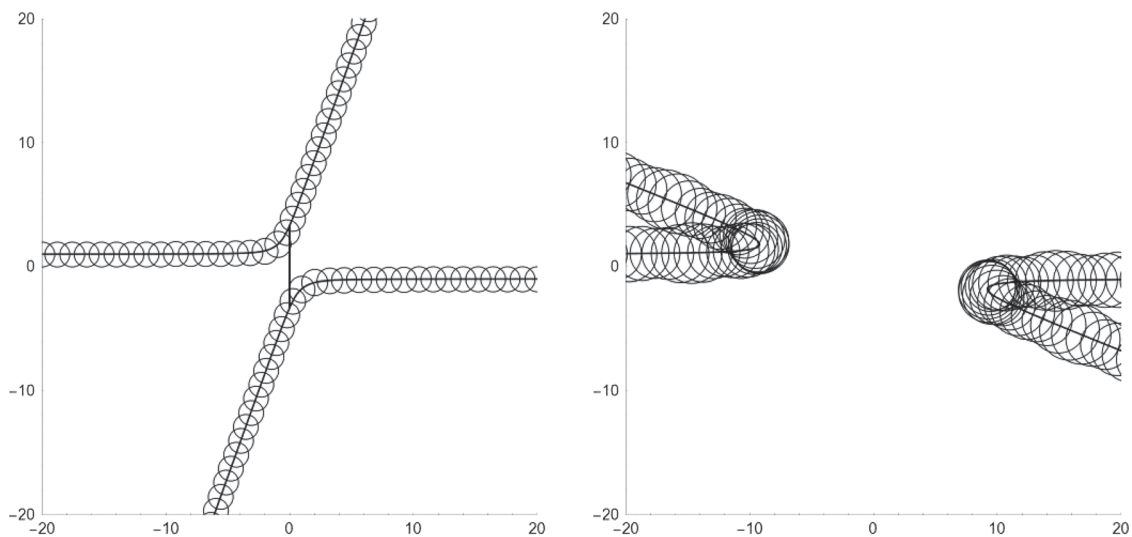


FIG. 10. Plot of dyonic-instanton scattering for $b = -1$, $|q| = 0.1$, $\zeta = 0$ (above), $\zeta = 1$ (below). Note the visible oscillations on the right-hand graph.

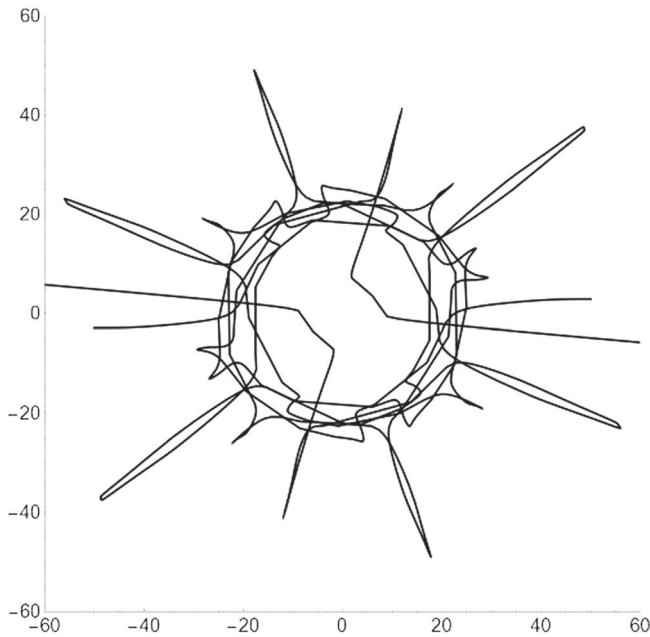


FIG. 11. Graph of scattering with orbiting behavior with $\zeta = 0.5$, $b = 0.5$, $q = 0.00438$.

We then moved on to looking at b ; here, there was similar behavior. At low ζ there did not seem to be any overall pattern, however increasing ζ led to graphs having a linear pattern, as in Fig. 12. This seems to be two examples of the same phenomenon, with very different scaling caused by the differences in the relative values of ζ . The magnitude of q did not seem to have a major effect on whether any linear pattern in the behavior was observed past a certain point, but continuing to make ζ larger caused the nonlinear behavior to return. Finally, we did not find any discernible patterns for $\dot{\theta}$ or $\dot{\rho}$ either. This difference as compared to the pure case is probably because the potential prevents the instanton size from growing large in the dyonic case, and therefore the transition to orthogonal scattering cannot occur.

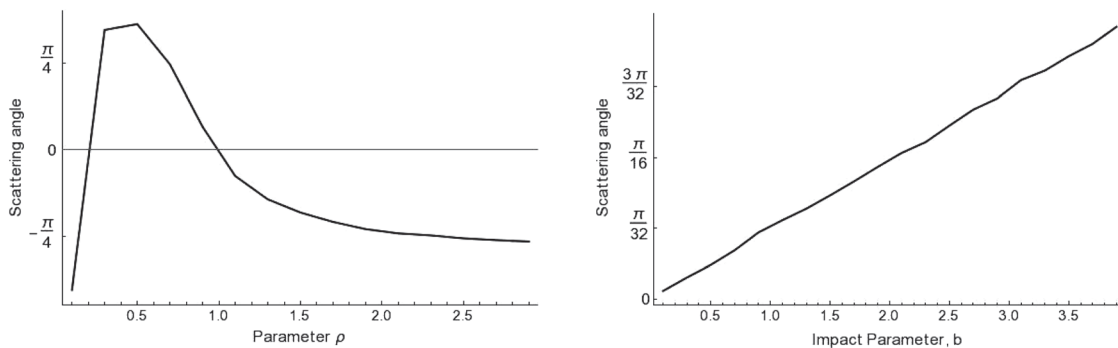


FIG. 12. Left: Scattering angle vs parameter ρ for $\zeta = q = 0.1$. As discussed in the text, we expect ρ to be a good approximation to the true initial size after the peak. Right: Scattering angle vs impact parameter for $\zeta = q = 0.5$. The case $b = 0$ is discussed in Fig. 8 and not included in this graph.

C. The six-parameter space

We now move on to look at the full six-parameter space, where the instantons are free to have different sizes and to vary in their gauge angle. The additional parameters add greatly to the complexity of the numerics. Due to this it is no longer possible to use the numerical algorithm from [13] as we had in the four-parameter case and so we had to use a new algorithm to produce the figures in this section.

There are two parameters to examine here. These are the relative gauge angle ϕ and the relative sizes of the instantons. Unless otherwise stated, the initial conditions for $\{\rho_1, \rho_2, \theta, x\}$ take the values $\{1, 1, 0, 50\}$, and the initial derivatives of all parameters are zero, except $\dot{x} = -0.03$. In the noncommutative case it is tricky to systematically explore the latter as the instanton sizes are nonlinear functions of ζ and the ρ_i . Therefore we chose to keep ζ fixed to set the overall length scale, and to vary the impact parameter rather than the instanton size, looking at cases where the separation was much smaller than, larger than and of the same order as the sizes of the instantons. Initially we kept the instantons the same size. We then checked the behavior in three cases $\rho_1 < b < \rho_2$, $b < \rho_1 < \rho_2$, and $\rho_1 < \rho_2 < b$.

In the commutative case, varying the gauge angle produces a clear sinusoidal variation (Fig. 13). This pattern held for different values of the impact parameter, however when the impact parameter was small compared to the instanton size, the variation takes on more of a ‘square’ shape (Fig. 13). As can be seen both from these two figures and from the scattering angles in Fig. 16, at $\phi = n\pi$, where the instantons are parallel in the gauge group, the interaction between the instantons disappears and they just move past one another. Conversely, the instantons interact most strongly at $\phi = n\pi + \pi/2$, where they are orthogonal in the gauge group. Changing the relative sizes of the instantons did not seem to affect this sinusoidal behavior, but it did change the strength of the interaction, with the scattering angle decreasing when the instantons were

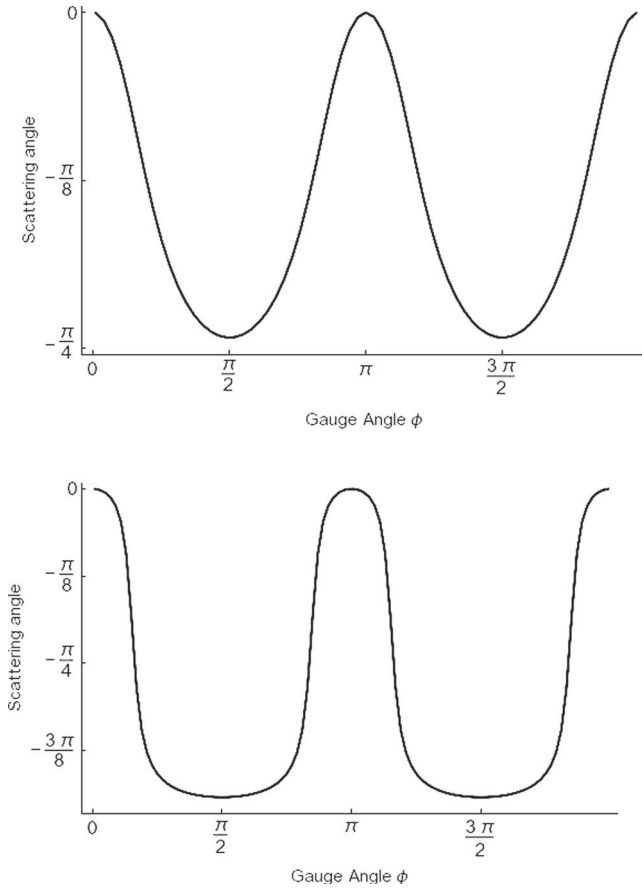


FIG. 13. Left: Graph of varying scattering angle ϕ with $\zeta = 0$, $\rho_1 = \rho_2 = 1$ and $b = 0.5$. Right: Graph of varying scattering angle ϕ with $\zeta = 0$, $\rho_1 = \rho_2 = 1$ and $b = 0.1$.

different sizes, with smaller sizes making the scattering angle smaller (Fig. 14).

The behavior in the noncommutative case is not so simple. The outline of the sinusoidal pattern is still present, but it is significantly disrupted, as in Fig. 15. Increasing the impact parameter somewhat restores the behavior (Fig. 15). There is therefore much less variation in the scattering angle for the noncommutative case. The instantons also no longer stop interacting when they are parallel in the gauge group, instead oscillating between minimum and maximum scattering angles, as in Fig. 15. Making one of the instantons smaller than the other and the impact parameter did not seem to have too much of an effect; however, making one larger than the impact parameter further disrupted the sinusoidal pattern, as in Fig. 17.

D. Conclusions

We end this section by reviewing the main results. We looked at both the full six-parameter space, and also a four-parameter subspace where the instantons were orthogonally embedded in the gauge group. This was necessary to analyze the dyonic case. Overall, increasing the noncommutative parameter ζ increases the repulsion between the

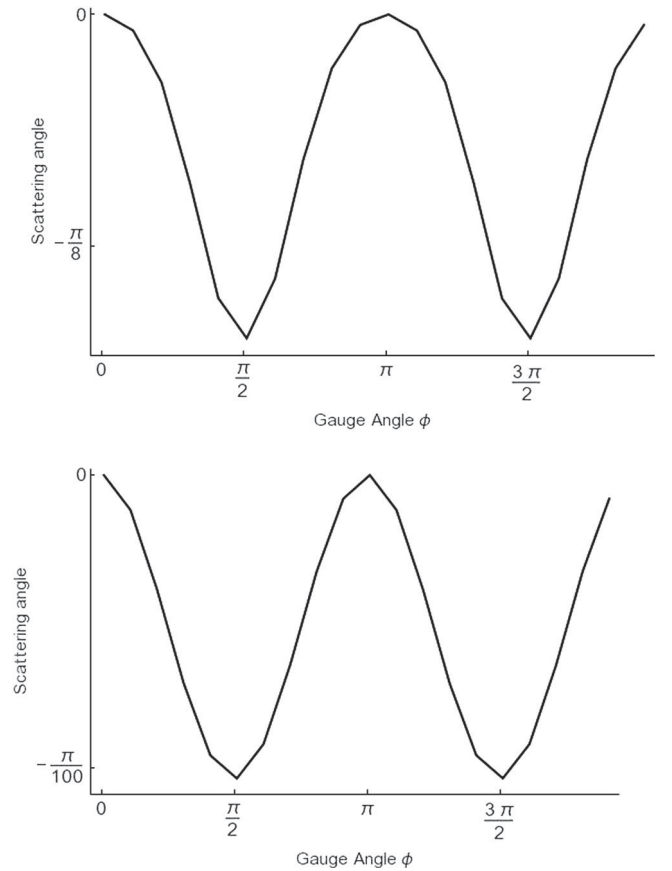


FIG. 14. Graph showing variation of scattering with gauge angle ϕ , where $\zeta = 0$ and $b = 0.5$. In both graphs $\rho_1 = 1$. In the left graph, $\rho_2 = 5$, and in the right graph $\rho_2 = 0.1$. Note that the scattering angle is much smaller in this case.

instantons. The form this takes is not straightforward, and in the pure instanton case involves a peak with strange behavior which requires a future, more detailed analysis with more sophisticated simulations. However, in general, even if the instantons begin by not interacting, they move from glancing off each other, to reflecting entirely as the parameter ζ increases.

We also found that orthogonal scattering was present in the noncommutative case as well as the commutative case. Systematically looking at the other parameters, we saw that, as expected, increasing ρ strengthens the repulsive effect of the scattering, and increasing the separation b decreases it. Further interesting behavior was observed seeing how the scattering changed when the quantities $\dot{\rho}$ and $\dot{\theta}$ were varied. For any nonzero value of these initial velocities, the scattering rapidly became almost orthogonal. This seems to be because making these parameters nonzero causes a rapid increase in the instanton size, and hence a very strong interaction.

This behavior is not found in the dyonic case; probably because the presence of the potential suppresses the instanton size. In the dyonic case there was the additional feature of orbiting behavior, some of a high winding number and great complexity.

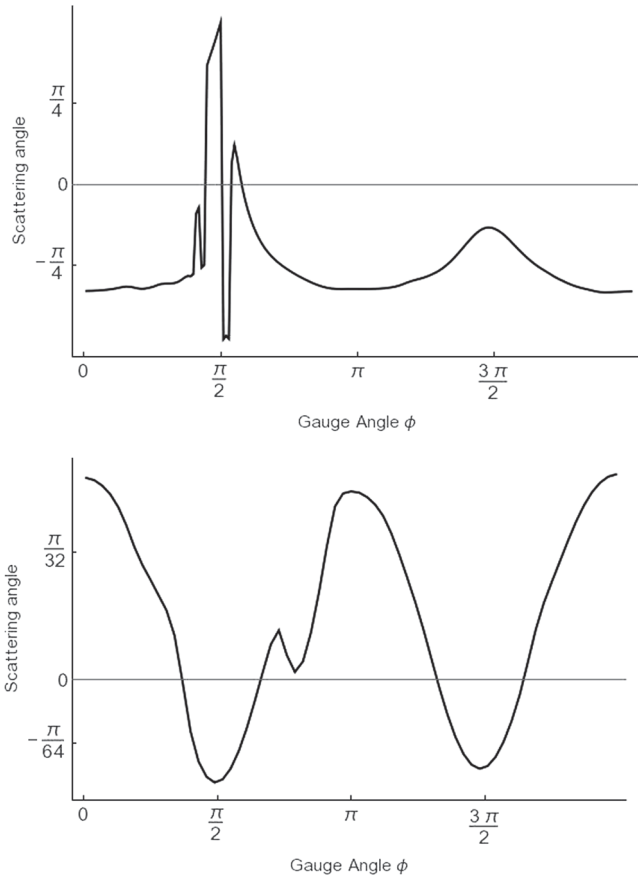


FIG. 15. Left: Graph showing variation of scattering angle ϕ with $\zeta = 1, \rho_1 = \rho_2 = 1$, and $b = 0.5$. The true instanton size is therefore $\sqrt{2}$, and so is roughly comparable to the separation. The splitting of the left peak appears to be a numerical error. Right: Graph showing variation of scattering angle ϕ with $\zeta = 1, \rho_1 = \rho_2 = 1$, and $b = 4$. The true instanton size is therefore $\sqrt{2}$, and so is much smaller than the separation. Note that the sinusoidal form is much more preserved, but now oscillates around zero rather than away from it.

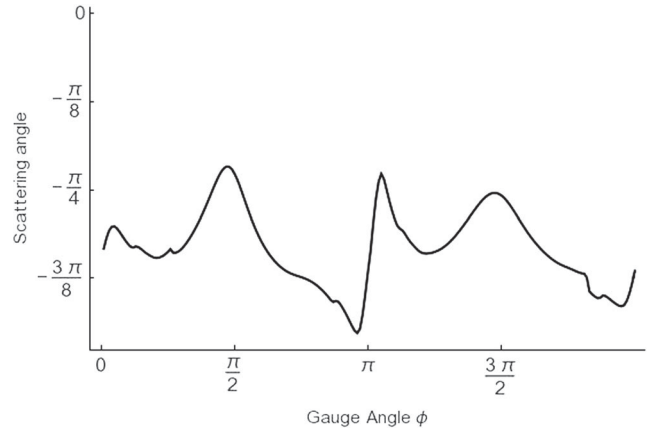


FIG. 17. Graph showing varying gauge angle ϕ with $\zeta = 1, \rho_1 = 1, \rho_2 = 5$, and $b = 0.5$. The true instanton sizes are $\sqrt{2}$ and just over 25 respectively.

Finally, we were able to use the six-parameter pure instanton case to analyze changing the gauge embedding. In general we found that the scattering oscillated with the gauge angle, but that this was suppressed as ζ was increased.

VI. THREE INSTANTONS

We now move on to the case of three instantons in SU(2) Yang-Mills. Here we only consider a commutative background, not a noncommutative one. We also use the usual version of the commutative ADHM construction with the quaternions rather than the biquaternion construction outlined above. As before, we begin by solving the ADHM constraints. We then calculate the scalar field for the dyonic case and use this to calculate the moduli space potential. Finally, we calculate the moduli space metric. The results in this section are original. There is, however, some related work in [28] and its related papers. There, some three

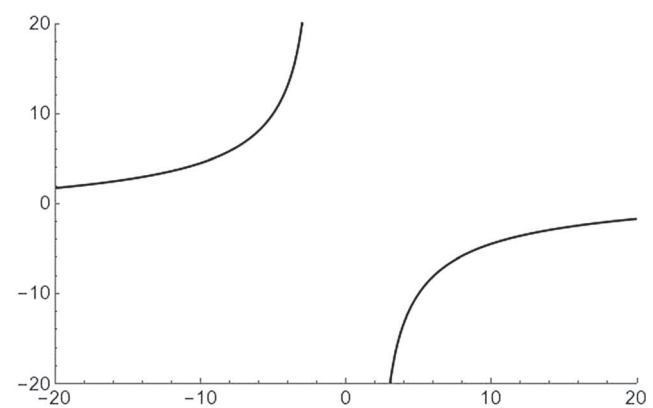
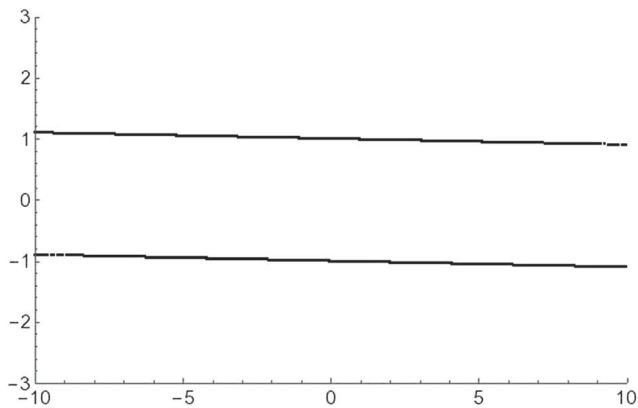


FIG. 16. Graph showing scattering examples from Fig. 15, with $\phi = \pi$ left and $\phi = 3\pi/2$ right. Note that the scales are different on the two graphs, and that the behavior is extremely different.

monopole solutions are found, using two methods involving writing the solution as a reduction of the ADHM equations. The first method is to use the Jackiw-Nohl-Rebbi (JNR) ansatz. This corresponds to taking Ω to be diagonal in our notation. The second is to calculate axial monopoles using ADHM data which has axial symmetry imposed on it via the Manton-Sutcliffe method. In our notation, there is a nondiagonal but specific form for Ω , and the instanton size v is chosen to be zero. These specific symmetries do not seem to match the ones we have chosen, and hence it not immediately clear how the results in that work relate to those presented here, but it would be interesting and worthwhile to pursue this in future.

Since we are in the commutative case, we need to solve the equation $\Delta^\dagger \Delta = 0$. For three instantons in SU(2) Yang-Mills, the ADHM data Δ is

$$\begin{bmatrix} \Lambda \\ \Omega \end{bmatrix} = \begin{bmatrix} u & v & w \\ \tau_1 & \sigma_1 & \sigma_2 \\ \sigma_1 & \tau_2 & \sigma_3 \\ \sigma_2 & \sigma_3 & \tau_3 \end{bmatrix}, \quad (66)$$

where the entries of Δ all lie in \mathbb{H} . With Δ as given above, we have three equations, one for each basis vector of $\mathfrak{o}(3)$. These are

$$\begin{aligned} \text{Im}_{\mathbb{H}}(\bar{u}v + (\bar{\tau}_1 - \bar{\tau}_2)\sigma_1 + \bar{\sigma}_2\sigma_3) &= 0, \\ \text{Im}_{\mathbb{H}}(\bar{u}w + (\bar{\tau}_1 - \bar{\tau}_3)\sigma_2 + \bar{\sigma}_1\sigma_3) &= 0, \\ \text{Im}_{\mathbb{H}}(\bar{v}w + (\bar{\tau}_2 - \bar{\tau}_3)\sigma_3 + \bar{\sigma}_1\sigma_2) &= 0. \end{aligned} \quad (67)$$

Note that these are now nonlinear in the ADHM data. Again, we were unable to find a solution on the full quaternion moduli space; however, if we restrict to the complex subspace as in the noncommutative two-instanton case, and use the three residual symmetries to set the real parts of the σ_i to zero, the terms in $\text{Im}(\bar{\sigma}_i\sigma_j)$ vanish, and we can solve as

$$\begin{aligned} \sigma_1 &= \frac{\tau_1 - \tau_2}{|\tau_1 - \tau_2|^2} (\alpha - \text{Im}_{\mathbb{C}}(\bar{u}v)), \\ \sigma_2 &= \frac{\tau_1 - \tau_3}{|\tau_1 - \tau_3|^2} (\beta - \text{Im}_{\mathbb{C}}(\bar{u}w)), \\ \sigma_3 &= \frac{\tau_2 - \tau_3}{|\tau_2 - \tau_3|^2} (\gamma - \text{Im}_{\mathbb{C}}(\bar{v}w)). \end{aligned} \quad (68)$$

For constants $\alpha, \beta, \gamma \in \mathbb{R}$, these are then constrained by the condition $\text{Re}_{\mathbb{C}}(\sigma_i) = 0$ to be

$$\begin{aligned} \alpha &= -\frac{\text{Im}_{\mathbb{C}}(\tau_1 - \tau_2)\text{Im}_{\mathbb{C}}(\bar{u}v)}{\text{Re}(\tau_1 - \tau_2)}, \\ \beta &= -\frac{\text{Im}_{\mathbb{C}}(\tau_1 - \tau_3)\text{Im}_{\mathbb{C}}(\bar{u}w)}{\text{Re}(\tau_1 - \tau_3)}, \\ \gamma &= -\frac{\text{Im}_{\mathbb{C}}(\tau_2 - \tau_3)\text{Im}_{\mathbb{C}}(\bar{v}w)}{\text{Re}(\tau_2 - \tau_3)}. \end{aligned} \quad (69)$$

The minus sign comes from the fact that each $\text{Im}_{\mathbb{C}}$ comes with a σ_3 , which multiply together to give -1 . The above equations give a solution for the complex subspace. As with the two-instanton case, the solutions for the scalar field, metric and potential are long and are given in Appendix F.

A. Three-instanton dynamics

The next step is to analyze the dynamics numerically, as was done in the case of two instantons. Unfortunately, we were unable to generate enough simulations to carry out a full analysis; however, we were able to observe some particular behaviors by plotting the scalar field profiles. When the instantons are far separated, this gives three peaks at the positions of each instanton, with the position defined as τ_i (Fig. 18). This confirms the interpretation of that parameter. If we move one instanton far away from the others (off to the right of the plot, in fact) then we see two peaks which look very similar to the graphs for two commutative instantons found in [13]. As the splitting in the right peak increases the closer the third instanton gets. In the graph in question, the two instantons shown are at $(\pm 1, 0)$ and the third is at $(0, 40)$. Finally, we were able to approximate some aspects of the scattering by plotting the

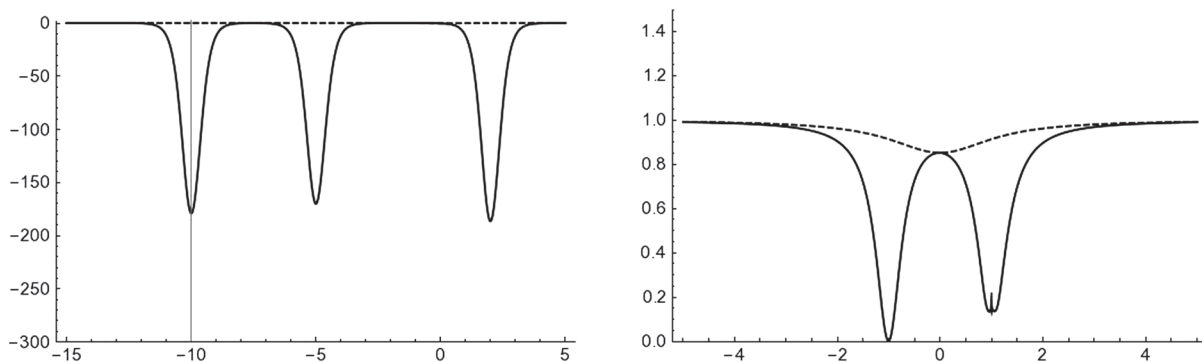


FIG. 18. (left) Plot of the scalar field profile for three separated instantons. (right) Plot of the scalar field profile for two instantons, with the third far separated off to the right.

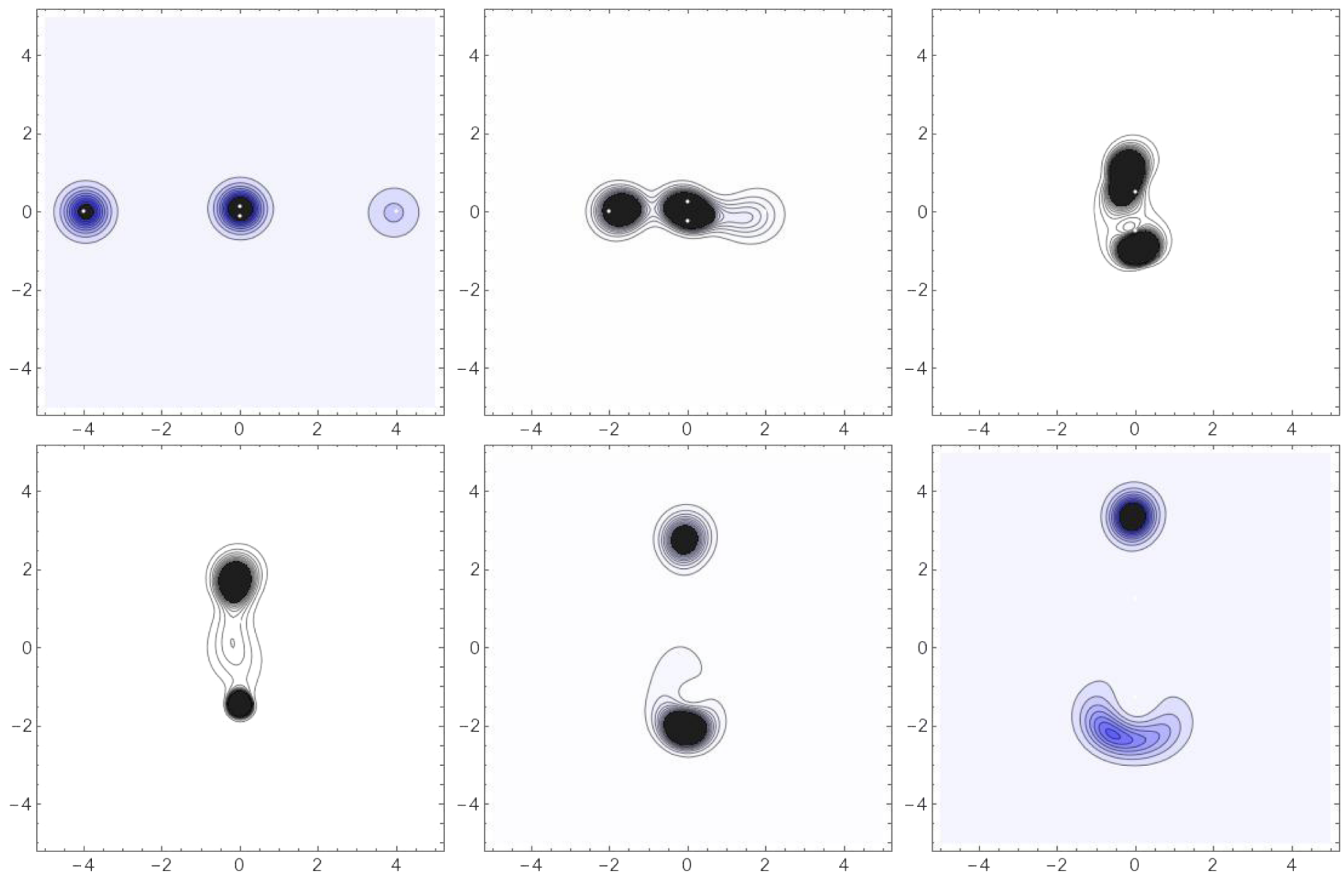


FIG. 19. Plot of the topological charge density with one instanton at the origin and the other two at decreasing values of τ_i . Note the apparent right angled scattering.

topological charge density (Fig. 19). Here, if one instanton is kept, ‘stationary’ at the origin, and the other instantons are plotted at successively closer values of τ_i , there appears to be the kind of right-angled scattering that is a familiar part of soliton dynamics. The fact that the instantons are moving away at very small values of τ_i is a function of the fact that the position depends both upon τ_i and σ_i , as in the two instanton case.

VII. CONCLUSION

We have presented a new notation and method for working with noncommutative ADHM instantons, by writing them explicitly in terms of biquaternion components. After deriving the form of the ADHM equation, as well as the moduli space and potential, for general $SU(2)$ instanton number in this notation, we attempted to solve them for the two-instanton case.

First, we rederived the commutative solution which was found in [13], but using biquaternions rather than quaternions. We were unable to find a solution on the full subspace but we were able to find one for the subspace of the moduli space spanned by the $\mathbb{C} \times \mathbb{C}$ subalgebra of $\mathbb{C} \times \mathbb{H}$. We used this solution to calculate the metric and potential for that subspace, and checked its behaviors in various limits.

Once we had these two solutions, we investigated the dynamics on the noncommutative moduli space numerically. In general, increasing the value of the noncommutative parameter ζ increased the repulsion between the instantons. However, the addition of the potential suppressed the repulsive force, particularly for large ζ .

Finally, we looked at the case of three $U(2)$ instantons. Again, we were able to find a solution on the submanifold of the moduli space spanned by the \mathbb{C} subgroup of \mathbb{H} . This solution once more allowed us to calculate the metric and potential on that submanifold, and to numerically graph the scalar field profiles. These solutions were very challenging numerically—however, the limited results we got indicated the presence of right-angled scattering, and the appropriate behavior of the solution in various limits. In terms of further work, the most obvious thing to do is to try and improve the efficiency of the numerical evaluations so that we can explore the dyonic six-parameter case for the noncommutative two instantons, and to access more of the three particle scattering in the three-instanton case. Analytically, we could try and extend our ADHM solutions from the subspaces of the moduli spaces to the full moduli spaces.

This would allow us to use the moduli space to calculate the number of BPS states in this topological sector, by

calculating a specific Witten index [29] on the moduli space. As argued in [29] the index is invariant under changes of the parameters of a theory, provided that these changes can be expressed as a conjugation of the supersymmetric variables in the theory, as such a conjugation leaves the supersymmetry properties of a theory unchanged. The moduli space potential is one of these parameters.

In [30] it is argued that the Dirac operator on the moduli space goes as $\exp(-q)$, where q is the absolute value of the moduli space potential, outside of small regions around the zeros of that potential. It is shown that rescaling the potential does not change the Witten index, so the number of BPS states remains the same in the limit that $q \rightarrow \infty$. In this limit the moduli space dynamics are exponentially suppressed outside of the small regions around the zeros. On the commutative moduli space this procedure cannot be carried out due to the presence of singularities, but because these singularities are removed by the multiplicity, in this case these regions should be describable by supersymmetric harmonic oscillators, as was found to be the case in [18] for single U(2) instantons. Calculating the Witten index, and hence the number of BPS states, would then be fairly straightforward. Therefore a key goal for future research would be to find the full moduli space and take the potential to infinity. This would suppress the dynamics everywhere except from regions of a small radius around the zeros of the potential, where it would be described by a supersymmetric quantum mechanics, for which we could calculate the Witten index, and hence the partition function. Once we have calculated this function, we can compare it to the result directly calculated from the field theory in [31]. This would provide a check for the $k=2$ case of the hypothesis mentioned in the introduction, where the (2,0) theory describing the interaction of multiple M5 branes is the strong coupling completion of 5D super Yang-Mills. If this is true, then the instantons of topological charge k should match with states of Kaluza-Klein momentum k around the circle of compactification, as explained in [32]. The $k=2$ section of the partition function for Kaluza-Klein states was calculated in [31], and so comparing this to the partition function on the instanton moduli space would be an important next step in verifying this conjecture.

ACKNOWLEDGMENTS

D. J. S. was supported in part by STFC Consolidated Grants ST/P000371/1 and ST/T000708/1. C. J. R. was supported by an STFC Studentship. J. A. F. was supported by an EPSRC Studentship.

APPENDIX A: SOLVING THE ADHM EQUATIONS

As stated in Eq. (51) the noncommutative ADHM equations are

$$\begin{aligned} 2\text{Im}_{\mathbb{H}}(\bar{\sigma}_R\sigma_I) - \text{Im}_{\mathbb{H}}(\bar{w}_R w_I)\text{Im}_{\mathbb{H}}(\bar{v}_R v_I) &= 0, \\ \text{Im}_{\mathbb{H}}(\bar{w}_R w_I) + \text{Im}_{\mathbb{H}}(\bar{v}_R v_I) &= -4\zeta\sigma_3, \\ \text{Im}_{\mathbb{H}}(\bar{\tau}\sigma_I) &= \frac{\text{Im}_{\mathbb{H}}(\bar{w}_R v_I + \bar{v}_R w_I)}{2} \equiv \frac{\Upsilon}{2}, \\ \text{Im}_{\mathbb{H}}(\bar{\tau}\sigma_R) &= \frac{\text{Im}_{\mathbb{H}}(\bar{w}_R v_R + \bar{w}_I v_I)}{2} \equiv \frac{\Lambda}{2}, \end{aligned} \quad (\text{A1})$$

where σ_3 is the quaternion basis element

$$\begin{bmatrix} i & 0 \\ 0 & -i \end{bmatrix}. \quad (\text{A2})$$

We can solve the third and fourth equations as

$$\sigma_R = \frac{\tau}{|\tau|^2} \left(\alpha + \frac{\Lambda}{2} \right) \quad (\text{A3})$$

and

$$\sigma_I = \frac{\tau}{|\tau|^2} \left(\gamma + \frac{\Upsilon}{2} \right). \quad (\text{A4})$$

We can use the second equation to deduce that

$$\bar{w}_R w_I = \beta - \bar{v}_R v_I - 4i\zeta\sigma_3, \quad (\text{A5})$$

and so

$$w_I = \frac{w_R\beta - w_R\bar{v}_R v_I - 4i\zeta w_R\sigma_3}{|w_R|^2}. \quad (\text{A6})$$

We want 12 independent real parameters, or three independent quaternion ones. We therefore aimed to solve for the other parameters in terms of v_R , w_R , and τ . We were unable to find a solution to these equations for the full biquaternion moduli space. However, we were able to find a solution on a complex valued geodesic submanifold. This subspace comes from restricting the quaternions to the subspace consisting of elements $z \in \mathbb{C}$ written as $x + y\sigma_3$, for $x, y \in \mathbb{R}$ and σ_3 is given by

$$\sigma_3 = \begin{bmatrix} i & 0 \\ 0 & -i \end{bmatrix}. \quad (\text{A7})$$

Note that $\sigma_3^2 = -\mathbb{1}_{\mathbb{H}}$, and therefore σ_3 can play the role of the imaginary unit. We start with the second ADHM equation, now for complex variables

$$\text{Im}_{\mathbb{C}}(\bar{v}_R v_I) + \text{Im}_{\mathbb{C}}(\bar{w}_R w_I) = -4\zeta\sigma_3. \quad (\text{A8})$$

Recall that we are using the notation $\text{Im}_{\mathbb{H}}$ to mean the imaginary quaternion part of an element of \mathbb{H} ; e.g., for $q = q_0 + \mathbf{q} \in \mathbb{H}$,

$$\text{Im}_{\mathbb{H}}(q) = \mathbf{q}. \quad (\text{A9})$$

On the other hand, $\text{Im}_{\mathbb{C}}$ takes the imaginary component of an element of \mathbb{C} . If $z \in \mathbb{C}$; $z = a + ib$

$$\text{Im}_{\mathbb{C}}(z) = b. \quad (\text{A10})$$

With these definitions in mind, we can solve this for w_I and v_I in terms of the other variables by finding a particular solution, then by adding the null space, found by solving

$$\text{Im}_{\mathbb{C}}(\bar{v}_R v_I) + \text{Im}_{\mathbb{C}}(\bar{w}_R w_I) = 0. \quad (\text{A11})$$

A particular solution is given by

$$v_{Ip} = \frac{-2\zeta v_R \sigma_3}{|v_R|^2}; \quad w_{Ip} = \frac{-2\zeta w_R \sigma_3}{|w_R|^2}. \quad (\text{A12})$$

We already know the solution to the null equation; it is

$$\tilde{v}_I = \frac{v_R}{|v_R|^2}(\beta - \bar{w}_R \tilde{w}_I). \quad (\text{A13})$$

For arbitrary real β and arbitrary quaternion \tilde{w}_I . Therefore, we have the general solution

$$\begin{aligned} v_I &= \frac{-2\zeta v_R \sigma_3}{|v_R|^2} + \frac{v_R}{|v_R|^2}(\beta - \bar{w}_R \tilde{w}_I), \\ w_I &= \frac{-2\zeta w_R \sigma_3}{|w_R|^2} + \tilde{w}_I. \end{aligned} \quad (\text{A14})$$

To complete this general solution we need to solve for \tilde{w}_I . This is done by solving the first ADHM equation

$$\text{Im}_{\mathbb{C}}(\bar{\sigma}_R \sigma_I) = \text{Im}_{\mathbb{C}}(\bar{v}_R v_I) - \text{Im}_{\mathbb{C}}(\bar{w}_R w_I). \quad (\text{A15})$$

We can use two of the symmetries in Eq. (54) to set $\text{Re}(\bar{\tau}\sigma) = 0$, by analogy to [13]. This corresponds to removing any component proportional to τ from σ . If we do this, then the equation becomes

$$-\frac{\text{Im}_{\mathbb{C}}(\Lambda\Upsilon)}{|\tau|^2} = \text{Im}_{\mathbb{C}}(\bar{v}_R v_I) - \text{Im}_{\mathbb{C}}(\bar{w}_R w_I). \quad (\text{A16})$$

If we now restrict to the complex plane spanned by $\mathbb{1}$ and σ_3 the left-hand side becomes zero, since Λ and Υ are both proportional to σ_3 , and hence their product is real and so $\text{Im}_{\mathbb{C}}(\Lambda\Upsilon) = 0$. Putting the solutions in (A14) into the right-hand side we get

$$\text{Im}_{\mathbb{C}}(\bar{w}_R \tilde{w}_I) = 0. \quad (\text{A17})$$

This leads to the solution

$$\begin{aligned} v_I &= \frac{-2\zeta v_R \sigma_3}{|v_R|^2} + B v_R, \\ w_I &= \frac{-2\zeta w_R \sigma_3}{|w_R|^2} + A w_R, \end{aligned} \quad (\text{A18})$$

for $A, B \in \mathbb{R}$. We can then use the remaining two symmetries to set A and B above to zero—see the discussion

below Eq. (54). Then we get the full solution for the complex subspace

$$\begin{aligned} v_I &= \frac{-2\zeta v_R \sigma_3}{|v_R|^2}, \\ w_I &= \frac{-2\zeta w_R \sigma_3}{|w_R|^2}, \\ \sigma_R &= \frac{\tau \text{Im}(\bar{w}_R v_R + \bar{w}_I v_I)}{2|\tau|^2} \\ &= \frac{(|v_R|^2 |w_R|^2 + 4\zeta^2)}{2|\tau|^2 |v_R|^2 |w_R|^2} \tau \text{Im}_{\mathbb{C}}(\bar{w}_R v_R) \sigma_3, \\ \sigma_I &= \frac{\tau \text{Im}_{\mathbb{C}}(\bar{w}_R v_I + \bar{v}_R w_I)}{2|\tau|^2} \\ &= -\frac{\zeta(|w_R|^2 + |v_R|^2)}{|\tau|^2 |v_R|^2 |w_R|^2} \tau \text{Im}_{\mathbb{C}}(\bar{w}_R v_R \sigma_3) \sigma_3. \end{aligned} \quad (\text{A19})$$

APPENDIX B: SOLVING THE SCALAR FIELD

The method outlined here is mainly based on Appendix 1 in [13], generalized to the case of arbitrary noncommutative instantons. That method is in turn based on [24]. It begins with the ansatz

$$\phi = iU^\dagger \mathcal{A} U; \quad \mathcal{A} = \begin{bmatrix} q & 0 \\ 0 & P \end{bmatrix}, \quad (\text{B1})$$

where ϕ is the scalar field we are trying to calculate and U is an element of the null space of the ADHM Matrix Δ . Further, $q \in u(N)$, where N is the degree of the instanton gauge group, and $P \in u(k)$, where k is the instanton number. In fact, iq is the VEV of the scalar field. For the real ADHM construction, we can use $o(k)$ rather than $u(k)$. In the biquaternion case in theory there is an additional $u(1)$, promoting the symmetry group to $u(2)$. In what follows we use our freedom to choose the VEV so that it lies in the $su(2)$ part of this overall $u(2)$.

Note that the equation for ϕ has the form of a rotation of \mathcal{A} by U . We can think of this as follows. The matrix \mathcal{A} belongs in $u(N) \times u(k)$. We can imagine it being defined on a $u(N) \times u(k)$ bundle over \mathbb{R}^4 . However we know the ADHM construction breaks the ‘gauge group’ $u(N) \times u(k)$ down to $u(N)$. We can therefore see the rotation as rotating \mathcal{A} into the $u(N)$ subspace picked out by the ADHM constraints. This interpretation can be confirmed by the straightforward observation that $U^\dagger(\mathbb{1} - UU^\dagger)\mathcal{A}U = 0$. A long and algebraic justification for the ansatz is given in [24]. Regardless of the justification for the ansatz, once we have it, the problem of solving for ϕ becomes the problem of solving for P above. It is shown in [24] that the equation of motion for ϕ

$$D^2\phi = 0 \quad (\text{B2})$$

expands as

$$D^2\phi = -4iU^\dagger\{bf b^\dagger, \mathcal{A}\}U + 4iU^\dagger b f \text{Tr}_2(\Delta^\dagger \mathcal{A} \Delta) f b^\dagger U = 0. \quad (\text{B3})$$

Here, Tr_2 refers to the quaternion trace on each element of a matrix, not to the trace of the matrix itself, which is written Tr . Hence, applied to a (complex/real) quaternion valued matrix, Tr_2 will give a complex/real valued matrix, whereas Tr will give a (complex/real) quaternion.

With \mathcal{A} written as above, the first term is $-4iU^\dagger\{f, p\}U$. For the second term, we recall that Δ can be written as

$$\Delta = \begin{bmatrix} \Lambda \\ \Omega - \mathbb{1}x \end{bmatrix}. \quad (\text{B4})$$

Writing $\Omega' = \Omega - \mathbb{1}x$, recalling that Ω and Ω' are Hermitian, and using the ADHM constraint $\Delta^\dagger \Delta = \Lambda^\dagger \Lambda + \Omega'^\dagger \Omega' = f^{-1}$ we can see

$$\begin{aligned} \text{Tr}_2(\Delta^\dagger \mathcal{A} \Delta) &= \text{Tr}_2(\Lambda^\dagger q \Lambda) + \text{Tr}_2(\Omega'^\dagger \mathcal{A} \Omega') \\ &= \text{Tr}_2(\Lambda^\dagger q \Lambda) + \frac{1}{2} \text{Tr}_2([\Omega'^\dagger, P] \Omega' - \omega'^\dagger [\Omega', P] + \{P, \Omega'^\dagger \Omega'\}) \\ &= \text{Tr}_2(\Lambda^\dagger q \Lambda) + \frac{1}{2} ([\Omega'^\dagger, P] \Omega' - \Omega'^\dagger [\Omega', P] + \{P, f^{-1}\} - \{P, \Lambda^\dagger \Lambda\}) \\ &= \text{Tr}_2(\Lambda^\dagger q \Lambda) + \frac{1}{2} (2\Omega'^\dagger P \Omega' - \{\Omega'^\dagger \Omega', P\} + \{P, f^{-1}\} - \{P, \Lambda^\dagger \Lambda\}). \end{aligned} \quad (\text{B5})$$

Now, note that x in the above expression is always the coefficient of $\mathbb{1}$. Therefore, the terms involving x in the above expression cancel, and we can everywhere replace Ω' by Ω [this is most easily seen from the third line of Eq. (B5)].

We can use these to rewrite (B3) as

$$D^2\phi = -4i \left(U^\dagger \left\{ f, P - \frac{1}{2} \text{Tr}_2(P) \right\} U + U^\dagger b f \left(\text{Tr}_2(\Lambda^\dagger q \Lambda) + \frac{1}{2} (2\Omega'^\dagger P \Omega' - \{\Omega'^\dagger \Omega', P\} - \{P, \Lambda^\dagger \Lambda\}) \right) \right). \quad (\text{B6})$$

Since P has complex components, not quaternion valued ones, $\text{Tr}_2(P) = P$ and the first term vanishes. Hence the equation of motion $D^2\phi = 0$ is equivalent to

$$\text{Tr}_2(\Lambda^\dagger q \Lambda) + \frac{1}{2} (2\Omega'^\dagger P \Omega' - \{\Omega'^\dagger \Omega', P\} - \{P, \Lambda^\dagger \Lambda\}) = 0. \quad (\text{B7})$$

This gives one equation for each component of P , allowing us to solve for P and hence, by extension, for ϕ .

APPENDIX C: CONSTRUCTING THE MODULI SPACE METRIC AND POTENTIAL

This section is based on Appendix 2 in [13], which is itself based on the method of [33] for calculating the metric determinant. This technique was adapted in [6] for the moduli space metric of two instantons, which they calculated to order $|\tau|^{-2}$. In [13] this is extended to the full metric for two commutative $U(2)$ instantons. We present the argument for arbitrary gauge group and topological charge.

As in Sec. III B, the metric on the moduli space is defined as

$$g_{rs} = \int d^4x \text{Tr}^*(\delta_r A_i \delta_s A_i), \quad (\text{C1})$$

where

$$\delta_r A_i = \partial_r A_i - D_i \epsilon_r \quad (\text{C2})$$

and

$$\text{Tr}^*(q) = \text{Tr}_2(\text{Tr}(q)). \quad (\text{C3})$$

There is one mode for each of the $8k$ moduli space coordinates, labeled here by the indices r and s . The index i refers to spacetime coordinates. Recall these zero modes are orthogonal to gauge transformations by definition

$$D_i(\delta_r A_i) = 0. \quad (\text{C4})$$

We can use this fact to find an explicit expression for the metric. First, we need an expression for $\partial_r A_i|_{z=z_0}$ in terms of the ADHM data. To do this, we recall that $A_i = U^\dagger \partial_i U$, and use the identity $U = PU$ with U the projection operator $\mathbb{1} - \Delta f \Delta^\dagger$ to derive

$$\partial_r U = -\Delta f \partial_r \Delta^\dagger U + P \partial_r U. \quad (\text{C5})$$

Using this result, the definition $A_i = U^\dagger \partial_i U$, and the product rule allows us to get the necessary result

$$\begin{aligned} \partial_r A_i|_{z=z_0} &= -iU^\dagger \partial_r \Delta f \bar{e}_i b^\dagger U + iU^\dagger b e_i f \partial_r \Delta^\dagger U \\ &\quad + D_i(iU^\dagger \partial_r U), \end{aligned} \quad (\text{C6})$$

around an arbitrary point of the moduli space z_0 . The zero mode is then this expression with the gauge dependent part removed. The third term above is explicitly a gauge transformation, however we also need to ensure that there is no gauge part implicit in the first two terms. To do this, we use the residual transformations described in Eq. (54) to transform the ADHM data as

$$\Delta \rightarrow q\Delta R, \quad U \rightarrow QU, \quad Q(z_0) = 1, \quad R(z_0) = 1. \quad (\text{C7})$$

It can be seen that this transformation leaves A_i invariant, and that

$$\begin{aligned} \partial_r A_i|_{z=z_0} &= -iU^\dagger C_r f \bar{e}_i b^\dagger U + iU^\dagger b e_i f C_r^\dagger U \\ &\quad + D(iU^\dagger \partial_r(Q^\dagger U)) \end{aligned} \quad (\text{C8})$$

with

$$C_r = \partial_r \Delta + \partial_r Q \Delta + \Delta \partial_r R. \quad (\text{C9})$$

It turns out we can choose C_r so that the first two terms of $\delta_r A_i$ have no gauge part—i.e., they are a zero mode. To do so we must prove the following:

Lemma C.1. If we choose C_r to be independent of x with

$$\Delta^\dagger C_r = (\Delta^\dagger C_r)^{T*} \quad (\text{C10})$$

the expression

$$\partial_r A_i = -iU^\dagger C_r f \bar{e}_i b^\dagger U + iU^\dagger b e_i f C_r^\dagger U \quad (\text{C11})$$

will be a zero mode.

To do this, we first note that the condition (C10) is equivalent to the two conditions

$$a^\dagger C_r = (a^\dagger C_r)^{T*}; \quad b^\dagger C_r = (b^\dagger C_r)^{T*}, \quad (\text{C12})$$

and then consider the expression (forming part of $\delta_r A_i$ above)

$$a_i := U^\dagger b f e_i. \quad (\text{C13})$$

We can then calculate

$$\begin{aligned} D_i a_j &= \partial_i a_j - iA_i a_j \\ &= U^\dagger e_i b f \Delta^\dagger b f e_j + U^\dagger b f (\bar{e}_i b^\dagger \Delta + \Delta^\dagger b e_i). \end{aligned} \quad (\text{C14})$$

We then write $\Delta^\dagger b$ in terms of its quaternion components as $c_k \bar{e}_k$, where the c_k are complex valued matrices. It is important to note that since $\Delta^\dagger b = \Omega$, the bottom $2k \times 2k$

part of the ADHM data, the c_k are hermitian, since Ω is Hermitian by construction. Keeping this fact in mind, we can write (C14) as

$$D_i a_j = U^\dagger b f c_k f (e_i \bar{e}_k e_j + \bar{e}_i e_k e_j + \bar{e}_k e_i e_j). \quad (\text{C15})$$

Now, we use the identity $\bar{e}_i e_j = -\bar{e}_j e_i + 2\delta_{ij}$ to get

$$D_i a_j = -U^\dagger b f c_k (e_i \bar{e}_j e_k - 2\delta_{jk} e_i - 2\delta_{ik} e_j). \quad (\text{C16})$$

Then we can see a_j satisfies both the linear self-dual field equation

$$D_{[i} a_{j]} = \frac{1}{2} \epsilon_{ijkl} a_k a_l \quad (\text{C17})$$

and the zero mode condition $D_i a_i = 0$. What does this say about the full mode $\delta_r A_i$? We calculate

$$\begin{aligned} D_i(\delta_r A_j) &= -iD_i U^\dagger C_r D_i a_j^\dagger + i a_j C_r^\dagger D_i U - iU^\dagger C_r (D_i a_j)^\dagger \\ &\quad + iD_i a_j C_r^\dagger U \\ &= -iU^\dagger b f (e_i \Delta^\dagger C_r \bar{e}_j - e_j C_r^\dagger \Delta \bar{e}_i) f b^\dagger U \\ &\quad - iU^\dagger C_r D_i a_j^\dagger + iD_i a_j C_r^\dagger U \\ &\quad - iU^\dagger C_r D_i a_j^\dagger + iD_i a_j C_r^\dagger U. \end{aligned} \quad (\text{C18})$$

Here we have used the fact that

$$D_i U^\dagger - iA_i U^\dagger = U^\dagger e_i b f \Delta^\dagger. \quad (\text{C19})$$

The discussion above of $D_i a_j$ shows that the last two terms of (C18) are a zero mode. We must therefore check the first two terms. The only parts of these which depend on the moduli space coordinates are

$$e_i \Delta^\dagger C_r \bar{e}_j - e_j C_r^\dagger \Delta \bar{e}_i \equiv K_{ij}. \quad (\text{C20})$$

So the first two terms being a zero mode are equivalent to

$$K_{[ij]} = \frac{1}{2} \epsilon_{ijkl} K_{kl}; \quad K_{ii} = 0 \quad (\text{C21})$$

and these are satisfied iff $\Delta^\dagger C_r = (\Delta^\dagger C_r)^{T*}$. This proves the above lemma. To use this result, we must see what this condition says about the form of C_r . First we define

$$C_r = \partial_r \Delta + \partial_r Q \Delta + \Delta \partial_r R, \quad (\text{C22})$$

$$Q = \begin{bmatrix} q & 0 \\ 0 & R^{-1} \end{bmatrix}, \quad (\text{C23})$$

Note that we can write C_r as

$$\partial_r a + \partial_r Q a + a \partial_r R + (\partial_r b + \partial_r Q b + b \partial_r R)x. \quad (\text{C24})$$

Next we set $q = 1$. This means it does not contribute to the variation of Q which means

$$\partial_r Q = -b\partial_r R b^\dagger. \quad (\text{C25})$$

(The conjugation by b is necessary to give $\partial_r Q$ the correct dimensions). Then we see that the part of C_r proportional to x is zero, since $\partial_r b$ is zero as b is a constant matrix and the other two terms cancel. This leaves us with

$$C_r = \partial_r a + \partial_r Q a + a \partial_r R. \quad (\text{C26})$$

With this form, and the fact that $R^{T^*} = -R$, since R is antiunitary, it is straightforward that $b^\dagger C_r = (b^\dagger C_r)^{T^*}$. The second condition, $a^\dagger C_r = (a^\dagger C_r)^{T^*}$ is satisfied if and only if

$$\begin{aligned} a^\dagger \partial_r a - (a^\dagger \partial_r a)^{T^*} - a^\dagger b \partial_r R b^\dagger a - (a^\dagger b \partial_r R b^\dagger a)^{T^*} \\ + a^\dagger a \partial_r R - (a^\dagger b \partial_r R b^\dagger a)^{T^*} = 0. \end{aligned} \quad (\text{C27})$$

We have therefore reduced the problem of finding the zero modes to solving the above equation.

The metric is then derived from the inner product of two zero modes. To find this, we use the following result from [33]

$$\text{Tr}^*(\delta_r A_i \delta_s A_i) = -\frac{1}{2} \partial^2 \text{Tr}^*(C_r^\dagger P C_s f + f C_r^\dagger C_s), \quad (\text{C28})$$

where $P = \mathbb{1} - \Delta f \Delta^\dagger$. We can then use Stoke's theorem to find the metric

$$\begin{aligned} g_{rs} &= -\frac{1}{2} \int_{\mathcal{M}} \partial^2 \text{Tr}^*(C_r^\dagger P C_s f + f C_r^\dagger C_s) \\ &= \int_{\partial \mathcal{M}} \text{Tr}^*(C_r^\dagger P_\infty C_s + C_r^\dagger C_s)_{ij} \\ &= 2\pi^2 \text{Tr}^*(C_r^\dagger P_\infty C_s + C_r^\dagger C_s)_{ij} \\ &= 2\pi^2 \text{Tr}^*(\partial_r a^\dagger (1 + P_\infty) \partial_s a - (a^\dagger \partial_r a - (a^\dagger \partial_r a)^T)_{ij} \partial_s R). \end{aligned} \quad (\text{C29})$$

Here

$$\begin{aligned} P_\infty &= \lim_{x \rightarrow \infty} P = \mathbb{1}_{n+2k \times n+2k} - b b^\dagger \\ &= \begin{bmatrix} \mathbb{1}_{n/2 \times n/2} & 0 \\ 0 & 0_{k \times k} \end{bmatrix} \end{aligned} \quad (\text{C30})$$

remembering that

$$\Delta(x) = \begin{bmatrix} \Lambda \\ \Omega + \tilde{\rho} \mathbb{1}_{k \times k} \end{bmatrix} - x \begin{bmatrix} 0 \\ \mathbb{1}_{k \times k} \end{bmatrix}. \quad (\text{C31})$$

(Note that the term in $\tilde{\rho}$ gives the center of mass, and is usually absorbed into the x component by a suitable choice of coordinates, but it is there, and therefore we consider it here—albeit briefly). The first term above then gives

$$2\pi^2 \text{Tr}^*(da^\dagger (1 + P_\infty) da) = 2\pi^2 \text{Tr}^*(2\Lambda^\dagger \Lambda + \Omega^\dagger \Omega + 2d\tilde{\rho}^\dagger d\tilde{\rho}). \quad (\text{C32})$$

The $d\tilde{\rho}^\dagger d\tilde{\rho}$ directions are flat and decouple from the rest of the metric and so we ignore them (They correspond to the position of the center of mass). This gives the first part of the metric

$$ds_1^2 = 2\pi^2 \text{Tr}^*(da^\dagger (1 + P_\infty) da) = 2\pi^2 \text{Tr}^*(2\Lambda^\dagger \Lambda + \Omega^\dagger \Omega). \quad (\text{C33})$$

Now for the second part of the metric

$$ds_2^2 = 2\pi^2 \text{Tr}^*((a^\dagger da - (a^\dagger da)^{T^*}) dR). \quad (\text{C34})$$

To find an explicit expression we write dR in terms of its components considered as a $U(k)$ matrix, and solve for them using (C27). We get one equation for each component, and solving them gives dR in terms of the ADHM parameters. We will see this explicitly in the specific cases below. Once we have done this, we can put all these parts together to get the full metric

$$\begin{aligned} ds^2 &= ds_1^2 + ds_2^2 = 2\pi^2 (\text{Tr}^*(da^\dagger (1 + P_\infty) da) \\ &= 2\pi^2 (\text{Tr}^*(2d\Lambda^\dagger d\Lambda + d\Omega^\dagger d\Omega) \\ &+ \text{Tr}^*((a^\dagger da - (a^\dagger da)^{T^*}) dR)), \end{aligned} \quad (\text{C35})$$

APPENDIX D: CONSTRUCTING THE POTENTIAL

We can use the metric to calculate the potential for the dyonic-instanton moduli space. This also makes use of the solution for the scalar field in Appendix B. Recall the definition of the potential

$$\mathcal{V} = \int d^4x \text{Tr}(D_i \phi D_i \phi). \quad (\text{D1})$$

Integrating by parts and using the fact that $D^2 \phi = 0$ via its equation of motion we get

$$\mathcal{V} = \lim_{R \rightarrow \infty} \int_{|x|=R} dS^3 \hat{x}_i \text{Tr}(\phi D_i \phi). \quad (\text{D2})$$

Using the facts that $\phi = U^\dagger \mathcal{A} U$, $D_i = \partial_i - iA_i$ and $A_i = U^\dagger \partial_i U$, a moderately long calculation [13] gives

$$D_i \phi = iU^\dagger e_i b f \Delta^\dagger \mathcal{A} U + iU^\dagger \mathcal{A} \Delta f \tilde{e}_i b^\dagger U. \quad (\text{D3})$$

To fully evaluate this integral, we need an expression for U . In general this would be rather complicated; however, we only need the value of U on the boundary, in the limit $R \rightarrow \infty$. For a general ADHM matrix

$$\begin{bmatrix} v_1 & v_2 & v_3 & \dots & v_k \\ \tau_1 - x & \sigma_1^* & \sigma_2^* & \dots & \sigma_{k-1}^* \\ \sigma_1 & \tau_2 - x & \sigma_k^* & \dots & \sigma_{2k-3}^* \\ \vdots & & \ddots & & \vdots \\ \sigma_{k-1} & \sigma_{2k-3} & \sigma_{3k-4} & \dots & \tau_k - x \end{bmatrix}, \quad (\text{D4})$$

the condition $\Delta^\dagger U = 0$ is solved to leading order in $|x|$ by

$$U_1 \mapsto 1; \quad U_i \mapsto \frac{x}{|x|^2} v_{i-1}^\dagger, \quad i \neq 1. \quad (\text{D5})$$

We might worry here about the issue discussed in Sec. III A, where U may or may not satisfy the completeness relation (35). In general we would need to worry about this, however if we expand in powers of ζ , any terms including a correction of order ζ^n would, by dimensional analysis, also have to go as $|x|^{-2n}$, and are therefore neglected in this limit. We also need these two results for the behavior of other quantities in this limit

$$\begin{aligned} \Delta &\mapsto \begin{bmatrix} \Lambda \\ -x \mathbb{1}_k \end{bmatrix}, \\ f &\mapsto \frac{1}{|x|^2} \mathbb{1}_k. \end{aligned} \quad (\text{D6})$$

We can use these to expand Eq. (D3), and then multiplying by \hat{x}_i we get, to leading order

$$\hat{x}_i D_i \phi = \frac{2i}{|x|^3} (q \Lambda \Lambda^\dagger - \Lambda P \Lambda^\dagger) + \mathcal{O}\left(\frac{1}{|x|^4}\right). \quad (\text{D7})$$

Remembering that $\phi = iq$ on the boundary, we can then write, to leading order

$$\begin{aligned} \mathcal{V} &= \lim_{R \rightarrow \infty} \int_{|x|=R} dS^3 \hat{x}_i \text{Tr}(\phi D_i \phi) \\ &= -2 \lim_{R \rightarrow \infty} \int_{|x|=R} dS^3 \frac{1}{|x|^3} (q^2 \Lambda \Lambda^\dagger - q \Lambda P \Lambda^\dagger) + \mathcal{O}\left(\frac{1}{|x|^4}\right) \\ &= -4\pi^2 \text{Tr}(q^2 \Lambda \Lambda^\dagger - q \Lambda P \Lambda^\dagger). \end{aligned} \quad (\text{D8})$$

Now we have these general expressions and methods for the ADHM solutions, moduli space metric, and potential, the following appendices will provide particular solutions for the cases discussed in the main text.

APPENDIX E: SCALAR FIELD, METRIC AND POTENTIAL IN THE TWO INSTANTON CASE

1. The scalar field

We begin with the scalar field. Following the method in Appendix B, we have the ansatz,

$$\phi = U^\dagger \mathcal{A} U; \quad \mathcal{A} = \begin{bmatrix} q & 0 \\ 0 & P \end{bmatrix}. \quad (\text{E1})$$

Here q is in the odd graded part of $\mathbb{C} \times \mathbb{H}$; i.e., $q = iq_0 + \mathbf{q}$, where $q_0 \in \mathbb{R}$ and $\mathbf{q} \in \text{Im}_{\mathbb{H}} \mathbb{H}$. The matrix P is anti-Hermitian, and so can be parametrized by

$$\begin{bmatrix} ai & ci - b \\ ci + b & di \end{bmatrix}. \quad (\text{E2})$$

The equation for the scalar field is

$$\begin{aligned} 2\text{Tr}_2(\Lambda^\dagger q \Lambda) + \text{Tr}_2([\Omega^\dagger, P] \Omega - \Omega^\dagger [\Omega, P]) \\ - \text{Tr}_2(\{P, \Lambda^\dagger \Lambda\}) = 0. \end{aligned} \quad (\text{E3})$$

Solving this equation is a lengthy calculation, which gives

$$\begin{aligned} a &= -\frac{1}{\Theta} (A(3)(g^2 N_{AI} - f^2 N_{AR}) + A(2)w(4gP - fN_{AR}) + A(1)w(4fP - gN_{AI}) \\ &\quad - ((16P^2 - N_{AR} N_{AI})(A(3)(2s + w) + wA(4))), \\ b &= \frac{1}{2\Theta} (A(1)(f^2(v + w) - 2N_{AI}(sv + sw + vw)) + A(2)(fg(v + w) + 8P(sv + sw + vw)) \\ &\quad + (4fP + gN_{AI})(A(3)(v - w) - A(4)(v + w))), \\ c &= \frac{1}{2\Theta} (A(1)(fg(v + w) - 8P(sv + sw + vw)) + A(2)(g^2(v + w) + 2N_{AR}(sv + sw + vw)) \\ &\quad + (fN_{AR} + 4gP)(A(3)(v - w) + A(4)(v + w))), \\ d &= -\frac{1}{\Theta} (A(3)(f^2 N_{AR} - g^2 N_{AI}) + A(2)v(4gP - fN_{AR}) + A(1)v(4fP - gN_{AI}) \\ &\quad + (A(3)(2s + v) - A(4)v)(16P^2 - XY)), \end{aligned} \quad (\text{E4})$$

where

$$\begin{aligned}
A(1) &= 4q_0 \text{Re}_{\mathbb{H}}(\bar{v}_R w_I - \bar{v}_I w_R) - 4 \text{Re}_{\mathbb{H}}(\bar{v}_R \mathbf{q} w_R + \bar{v}_I \mathbf{q} w_I), \\
A(2) &= 4q_0 \text{Re}_{\mathbb{H}}(\bar{v}_R w_R + \bar{v}_I w_I) + 4 \text{Re}_{\mathbb{H}}(\bar{v}_R \mathbf{q} w_I - \bar{v}_I \mathbf{q} w_R), \\
A(3) &= q_0(|v_R|^2 + |v_I|^2 - |w_R|^2 - |w_I|^2) + 2 \text{Re}_{\mathbb{H}}(\bar{v}_R q v_I - \bar{w}_R q w_I), \\
A(4) &= q_0(|v_R|^2 + |v_I|^2 + |w_R|^2 + |w_I|^2) + 2 \text{Re}_{\mathbb{H}}(\bar{v}_R v_I + \bar{w}_R q w_I), \\
f &= \text{Re}_{\mathbb{H}}(\bar{w}_R v_R + \bar{w}_I v_I), \\
g &= \text{Re}_{\mathbb{H}}(\bar{w}_I v_R - \bar{v}_I w_R), \\
x &= |\sigma_R|^2, \\
y &= |\sigma_I|^2, \\
P &= \text{Re}_{\mathbb{H}}(\bar{\sigma}_R \sigma_I), \\
v &= |v_R|^2 + |v_I|^2, \\
w &= |w_R|^2 + |w_I|^2, \\
N_{AR} &= |v_R|^2 + |v_I|^2 + |w_R|^2 + |w_I|^2 + 4(|\tau|^2 + |\sigma_R|^2), \\
N_{AI} &= |v_R|^2 + |v_I|^2 + |w_R|^2 + |w_I|^2 + 4(|\tau|^2 + |\sigma_I|^2), \\
\Theta &= (v + w)(f^2 N_{AR} - g^2 N_{AI}) + 2(16P^2 - N_{AR} N_{AI})(sv + sw + vw). \tag{E5}
\end{aligned}$$

In the commutative limit from [13], that is, $\zeta = 0$ and the imaginary quaternion parts q_I set to zero, this becomes

$$b = \frac{-2 \text{Re}_{\mathbb{H}}(\bar{v} \mathbf{q} w)}{\Sigma_+ + 4(|\tau|^2 + |\sigma_R|^2)}; \quad a, b, d = 0, \tag{E6}$$

which is precisely the result in that paper.

Another useful limit is that in which $|\tau| \mapsto \infty$. In this case

$$\begin{aligned}
a &= \frac{q_0(|v_R|^2 + |v_I|^2) + 2 \text{Re}(\bar{v}_R \mathbf{q} v_I)}{|v_R|^2 + |v_I|^2}, \\
d &= \frac{q_0(|w_R|^2 + |w_I|^2) + 2 \text{Re}(\bar{w}_R \mathbf{q} w_I)}{|w_R|^2 + |w_I|^2}. \tag{E7}
\end{aligned}$$

With $b, c = 0$. This corresponds to the two instantons being far separated. In this case we would expect them to look like two single U(2) instantons, and we see that we do in fact have two copies of the solution for a single instanton given in Sec. (IV A). The next step is to use this to explicitly calculate the potential.

2. The potential

Recall from Appendix D that the potential is given by

$$V = \int d^4 x \text{Tr}(D_i \phi D_i \phi). \tag{E8}$$

Integrating by parts, and using the equation of motion for ϕ

$$D^2 \phi = 0 \tag{E9}$$

we get

$$V = \lim_{R \rightarrow \infty} \int_{|x|=R} dS^3 \hat{x}_i \text{Tr}(\phi D_i \phi). \tag{E10}$$

We know that the vector U , being a null vector of Δ , must solve

$$\begin{aligned}
v^\dagger U_1 + (\tau^\dagger - x^\dagger) U_2 + \sigma^\dagger U_3 &= 0, \\
w^\dagger U_1 + \sigma^\dagger U_2 - (\tau^\dagger + x^\dagger) U_3 &= 0. \tag{E11}
\end{aligned}$$

This is solved on the boundary by

$$\begin{aligned}
U_1 &\mapsto 1, \\
U_2 &\mapsto \frac{x}{|x|^2} v^\dagger, \\
U_3 &\mapsto \frac{x}{|x|^2} w^\dagger. \tag{E12}
\end{aligned}$$

Solving these equations following the method in Appendix D is long, however eventually we get

$$\begin{aligned} \mathcal{V} = & 8\pi^2(|q|^2(|v_R|^2 + |v_I|^2 + |w_R|^2 + |w_I|^2) + 4q_0\text{Re}_{\mathbb{H}}(\bar{v}_R\bar{q}v_I + \bar{w}_R\bar{q}w_I) - a(q_0(|v_R|^2 + |v_I|^2 + 2\text{Re}_{\mathbb{H}}(\bar{v}_R\mathbf{q}v_I)) \\ & - d(q_0(|w_R|^2 + |w_I|^2) + 2\text{Re}_{\mathbb{H}}(\bar{w}_R\bar{q}w_I)) + 2b\text{Re}_{\mathbb{H}}(\bar{v}_R\bar{q}w_R + \bar{v}_I\bar{q}w_I) \\ & - 2bq_0\text{Re}_{\mathbb{H}}(w_I\bar{v}_R - w_R\bar{v}_I) - 2cq_0\text{Re}_{\mathbb{H}}(w_R\bar{v}_R + w_I\bar{v}_I) - 2c\text{Re}_{\mathbb{H}}(\bar{v}_R\bar{q}w_I - \bar{v}_I\bar{q}w_R)). \end{aligned} \quad (\text{E13})$$

We can choose the q_0 to be zero by requiring the VEV to lie in $SU(2)$. This simplifies our solution to

$$\begin{aligned} \mathcal{V} = & 8\pi^2(|q|^2(|v_R|^2 + |v_I|^2 + |w_R|^2 + |w_I|^2) - a(2\text{Re}(\bar{v}_R\mathbf{q}v_I)) - d(2\text{Re}(\bar{w}_R\bar{q}w_I)) \\ & + 2b\text{Re}(\bar{v}_R\bar{q}w_R + \bar{v}_I\bar{q}w_I) - 2c\text{Re}(\bar{v}_R\bar{q}w_I - \bar{v}_I\bar{q}w_R)), \end{aligned} \quad (\text{E14})$$

where a , b , c , and d are given above.

If instead we go back to the large τ limit, using (E7)

$$\begin{aligned} \mathcal{V} = & 8\pi^2 \left(|q|^2(|v_R|^2 + |v_I|^2 + |w_R|^2 + |w_I|^2) + 4q_0\text{Re}(\bar{v}_R\bar{q}v_I + \bar{w}_R\bar{q}w_I) \right. \\ & \left. - \frac{(q_0(|v_R|^2 + |v_I|^2 + 2\text{Re}(\bar{v}_R\mathbf{q}v_I)))^2}{|v_R|^2 + |v_I|^2} - \frac{(q_0(|w_R|^2 + |w_I|^2) + 2\text{Re}(\bar{w}_R\bar{q}w_I))^2}{|w_R|^2 + |w_I|^2} \right). \end{aligned} \quad (\text{E15})$$

In this case, the q_0 parts cancel explicitly, and we get

$$\mathcal{V} = 8\pi^2|\mathbf{q}|^2 \left(\hat{\mathbf{q}}(|v_R|^2 + |v_I|^2 + |w_R|^2 + |w_I|^2) - \frac{4\text{Re}^2(\bar{v}_R\hat{\mathbf{q}}v_I)}{|v_R|^2 + |v_I|^2} - \frac{4\text{Re}^2(\bar{w}_R\hat{\mathbf{q}}w_I)}{|w_R|^2 + |w_I|^2} \right). \quad (\text{E16})$$

We would expect this is the potential for two copies of the single U(1) instanton, and if we compare to the result in Sec. IV A we can easily see that this is the case.

3. The metric

As in Appendix C, we begin by calculating $a^\dagger\delta C_r$, and impose the condition

$$a^\dagger\delta C_r = (a^\dagger\delta C_r)^{T*}. \quad (\text{E17})$$

Once again, we carefully note that T involves taking the transpose considered as a 2×2 matrix of biquaternions. It

does not affect the quaternions themselves. The operation \star takes the complex conjugate of each element, which again does not affect the quaternions but only their complex coefficients.

We can expand δR in the $u(2)$ basis as

$$\delta R = \begin{bmatrix} id\phi & id\psi - d\theta \\ id\psi + d\theta & id\chi \end{bmatrix}. \quad (\text{E18})$$

This gives three simultaneous equations for the derivations in the different gauge directions. As discussed below Eq. (C34), we can use these along with Eq. (C27) to find δR in full

$$\begin{aligned} d\phi = & \frac{1}{\Phi} (-2B(1)(2s+w)(4fP - gN_{AI}) + 2B(2)((2s+w)(4gP - fN_{AR}) - (B(3)(2s+w) + B(4)w)(16P^2 - N_{AR}N_{AI}) \\ & - 2B(4)(f^2N_{AR} - 8fgP + g^2N_{AI})), \\ d\theta = & \frac{1}{\Phi} (2B(1)(f^2(4s+v+w) - N_{AI}(sv+sw+vw)) + 2B(2)(fg(4s+v+w) - 4P(sv+sw+vw)) \\ & + (B(3)(4s+v+w) - B(4)(v-w))(4fP - gN_{AI})), \\ d\psi = & \frac{1}{\Phi} (-2B(1)(fg(4s+v+w) - 4P(sv+sw+vw)) - 2B(2)(g^2(4s+v+w) - 2N_{AR}(sv+sw+vw)) \\ & + (B(3)(4s+v+w) - B(4)(v-w))(4gP - fN_{AR})), \\ d\chi = & \frac{1}{\Phi} (-2B(1)(2s+v)(4fP - gN_{AI}) + 2B(2)(2s+v)(4gP - fN_{AR}) \\ & - (16P^2 - N_{AR}N_{AI})(B(3)(2s+v) - B(4)v) + 2B(4)(f^2N_{AR} - 8fgP + g^2N_{AI})), \end{aligned} \quad (\text{E19})$$

where the terms are defined in (E5) with the addition of

$$\begin{aligned}
B(1) &= \bar{v}_R dw_R + \bar{v}_I dw_I - \bar{w}_R dv_R - w_I dv_I + 2(\bar{\tau} d\sigma_R - \bar{\sigma}_R d\tau), \\
B(2) &= \bar{v}_R dw_I - \bar{v}_I dw_R + \bar{w}_R dv_I - \bar{w}_I dv_R + 2(\bar{\sigma}_I d\tau - \bar{\tau} d\sigma_I), \\
B(3) &= \bar{v}_R dv_I - \bar{v}_I dv_R + \bar{w}_R dw_I - \bar{w}_I dw_R, \\
B(4) &= \bar{v}_R dv_I - \bar{v}_I dv_R - \bar{w}_R dw_I + \bar{w}_I dw_R + 2(\bar{\sigma}_R d\sigma_I - \bar{\sigma}_I d\sigma_R), \\
\Phi &= 4((4s + v + w)(f^2 X - 8fgP + g^2 Y) + (16P^2 - XY)(sv + sw + vw)).
\end{aligned} \tag{E20}$$

We can now use this in our formula (C35)

$$ds^2 = ds_1^2 + ds_2^2 = 2\pi^2(\text{Tr}^*(2d\Lambda^\dagger d\Lambda + d\Omega^\dagger d\Omega) + \text{Tr}^*((a^\dagger da - (a^\dagger da)^{T*})dR)). \tag{E21}$$

First we have that $a^\dagger da - (a^\dagger da)^{T*}$ is

$$\begin{aligned}
&\begin{bmatrix} 0 & \bar{v}_R dw_R + \bar{v}_I dw_I - \bar{w}_R dv_R - \bar{w}_I dv_I + 2(\bar{\tau} d\sigma_R - \bar{\sigma}_R d\tau) \\ -(\bar{v}_R dw_R + \bar{v}_I dw_I - \bar{w}_R dv_R - \bar{w}_I dv_I + 2(\bar{\tau} d\sigma_R - \bar{\sigma}_R d\tau)) & 0 \end{bmatrix} \\
&+ i \begin{bmatrix} 2(\bar{v}_R dv_I - \bar{v}_I dv_R + \bar{\sigma}_R d\sigma_I - \bar{\sigma}_I d\sigma_R) & \bar{v}_R dw_I - \bar{v}_I dw_R + \bar{w}_R dv_I - \bar{w}_I dv_R + 2(\bar{\sigma}_I d\tau - \bar{\tau} d\sigma_I) \\ \bar{v}_R dw_I - \bar{v}_I dw_R + \bar{w}_R dv_I - \bar{w}_I dv_R + 2(\bar{\sigma}_I d\tau - \bar{\tau} d\sigma_I) & 2(\bar{w}_R dw_I - \bar{w}_I dw_R - \bar{\sigma}_R d\sigma_I + \bar{\sigma}_I d\sigma_R) \end{bmatrix}.
\end{aligned} \tag{E22}$$

Once we have this it is fairly straightforward to calculate the metric as

$$\begin{aligned}
ds^2 &= 8\pi^2(d^2 v_R + d^2 v_I + d^2 w_R + d^2 w_I + d^2 \tau + d^2 \sigma_R + d^2 \sigma_I - \text{Re}_{\mathbb{H}}((\bar{v}_R dv_I - \bar{v}_I dv_R + \bar{\sigma}_R d\sigma_I - \bar{\sigma}_I d\sigma_R)d\phi \\
&\quad + (\bar{w}_R dw_I - \bar{w}_I dw_R - \bar{\sigma}_R d\sigma_I + \bar{\sigma}_I d\sigma_R)d\chi + (\bar{v}_R dw_R + \bar{v}_I dw_I - \bar{w}_R dv_R - \bar{w}_I dv_I + 2(\bar{\tau} d\sigma_R - \bar{\sigma}_R d\tau))d\theta \\
&\quad + (\bar{v}_R dw_I - \bar{v}_I dw_R + \bar{w}_R dv_I - \bar{w}_I dv_R + 2(\bar{\sigma}_I d\tau - \bar{\tau} d\sigma_I))d\psi).
\end{aligned} \tag{E23}$$

We can check the behavior of this solution in various limits. First of all, the commutative real limit, where the various imaginary quaternion parts q_I and the noncommutative parameter ζ are set to zero. In this limit we have

$$\begin{aligned}
d\phi &= d\psi = d\chi = 0; \\
d\theta &= \frac{\bar{v}_R dw_R - \bar{w}_R dv_R - \bar{w}_I dv_I + 2(\bar{\tau} d\sigma_R - \bar{\sigma}_R d\tau)}{|v_R|^2 + |w_R|^2 + 4(|\tau|^2 + |\sigma_R|^2)}.
\end{aligned} \tag{E24}$$

This allows us to calculate the metric to be

$$ds^2 = 8\pi^2 \left(d^2 v_R + d^2 w_R + d^2 \tau + d^2 \sigma_R - \frac{dk^2}{N_A} \right) \tag{E25}$$

with

$$\begin{aligned}
N_A &= |v_R|^2 + |w_R|^2 + 4(|\tau|^2 + |\sigma_R|^2), \\
dk &= \bar{v}_R dw_R - \bar{w}_R dv_R - \bar{w}_I dv_I + 2(\bar{\tau} d\sigma_R - \bar{\sigma}_R d\tau).
\end{aligned} \tag{E26}$$

exactly as in [13]. The second limit we can check is the limit in which $|\tau| \mapsto \infty$. Since this corresponds to the two instantons becoming far separated, in this limit we would

expect to get two copies of the solution for a single $U(2)$ instanton. In fact, we get

$$d\phi = \frac{v_R dv_I - \bar{v}_I dv_R}{|v_R|^2 + |v_I|^2}; \quad d\chi = \frac{w_R dw_I - \bar{w}_I dw_R}{|w_R|^2 + |w_I|^2}. \tag{E27}$$

This gives the metric

$$\begin{aligned}
ds^2 &= 8\pi^2 \left(d^2 v_R + d^2 v_I + d^2 w_R + d^2 w_I \right. \\
&\quad \left. - \frac{(v_R dv_I - \bar{v}_I dv_R)^2}{|v_R|^2 + |v_I|^2} - \frac{(w_R dw_I - \bar{w}_I dw_R)^2}{|w_R|^2 + |w_I|^2} \right).
\end{aligned} \tag{E28}$$

This is precisely the sum of two copies of the form in Sec. IV A above [Eq. (47)].

APPENDIX F: THREE INSTANTON METRIC AND POTENTIAL

1. The scalar field

As in the two-instanton case the expressions derived here for the scalar field, metric and potential are in principle valid for the full quaternion parametrization. However,

when we substitute in the solutions for the σ_i derived in Eq. (68), that is only valid for that particular complex subspace. Keeping this in mind, we use the same method as before. This time the ansatz is given by

$$\mathcal{A} = \begin{bmatrix} \mathbf{q} & 0 \\ 0 & P \end{bmatrix}, \quad (\text{F1})$$

where $\mathbf{q} \in su(2)$, and $P \in o(3)$, parametrized as

$$\begin{bmatrix} 0 & -a & b \\ a & 0 & -c \\ -b & c & 0 \end{bmatrix}. \quad (\text{F2})$$

The ADHM data Δ is given, in this case, by

$$\begin{bmatrix} u & v & w \\ \tau_1 & \sigma_1 & \sigma_2 \\ \sigma_1 & \tau_2 & \sigma_3 \\ \sigma_2 & \sigma_3 & \tau_3 \end{bmatrix}, \quad (\text{F3})$$

where $\tau_1 + \tau_2 + \tau_3 = 0$. Now the elements are all quaternions, not biquaternions. The equation we want to solve is still

$$2\text{Tr}_2(\Lambda^\dagger \mathbf{q} \Lambda) + \text{Tr}_2([\Omega^\dagger, P]\Omega - \Omega^\dagger[\Omega, P]) - \text{Tr}_2(\{P, \Lambda^\dagger \Lambda\}) = 0. \quad (\text{F4})$$

Proceeding as in the previous cases, we can solve for the components of \mathcal{A} as

$$\begin{aligned} a &= \frac{1}{\Upsilon} (C_3(2\Psi_2 M_{A2} - \Psi_1 \Psi_3) + C_2(2\Psi_1 M_{A3} - \Psi_2 \Psi_3) + C_1(-4M_{A2} M_{A3} - \Psi_3^2)), \\ b &= \frac{1}{\Upsilon} (-C_3(\Psi_1 \Psi_2 + 2M_{A1} z) + C_1(2\Psi_1 M_{A3} - \Psi_2 \Psi_3) - C_2(4M_{A1} M_{A3} - \Psi_2^2)), \\ c &= \frac{1}{\Upsilon} (-C_3(4M_{A1} M_{A2} - \Psi_1^2) - C_2(\Psi_1 \Psi_2 + 2M_{A1} \Psi_3) + C_1(2\Psi_2 Y - \Psi_1 \Psi_3)), \end{aligned} \quad (\text{F5})$$

where

$$\begin{aligned} C_1 &= 4\text{Re}_{\mathbb{H}}(\bar{v} \mathbf{q} u), \\ C_2 &= 4\text{Re}_{\mathbb{H}}(\bar{u} \mathbf{q} w), \\ C_3 &= 4\text{Re}_{\mathbb{H}}(\bar{w} \mathbf{q} v), \\ M_{A1} &= |u|^2 + |v|^2 + 3|\sigma_1|^2 + \Sigma^2 + |\tau_1 - \tau_2|^2, \\ M_{A2} &= |w|^2 + |v|^2 + 3|\sigma_2|^2 + \Sigma^2 + |\tau_1 - \tau_3|^2, \\ M_{A3} &= |w|^2 + |v|^2 + 3|\sigma_3|^2 + \Sigma^2 + |\tau_2 - \tau_3|^2, \\ \Psi_1 &= \text{Re}_{\mathbb{H}}(3(\bar{\tau}_1 \sigma_3 - \bar{\sigma}_2 \sigma_1) - \bar{w} v), \\ \Psi_2 &= \text{Re}_{\mathbb{H}}(3(\bar{\tau}_2 \sigma_2 - \bar{\sigma}_1 \sigma_3) - \bar{u} w), \\ \Psi_3 &= \text{Re}_{\mathbb{H}}(3(\bar{\tau}_3 \sigma_1 - \bar{\sigma}_3 \sigma_2) - \bar{v} u), \\ \Upsilon &= 2(\Psi_1^2 M_{A3} + \Psi_1 \Psi_2 \Psi_3 - 4M_{A1} M_{A2} M_{A3} \\ &\quad + M_{A1} \Psi_3^2 + \Psi_2^2 M_{A2}). \end{aligned} \quad (\text{F6})$$

2. The potential

We can now use this to calculate the potential, using the formula

$$V = \int d^4x \text{Tr}(D_i \phi D_i \phi). \quad (\text{F7})$$

We can now follow the standard method. Integrating by parts, and using the equation of motion for ϕ

$$D^2 \phi = 0. \quad (\text{F8})$$

We get

$$V = \lim_{R \rightarrow \infty} \int_{|x|=R} dS^3 \hat{x}_i \text{Tr}(\phi D_i \phi). \quad (\text{F9})$$

We know that the vector U , being a null vector of Δ , must solve $\Delta^\dagger U = 0$, which gives the equations

$$\begin{aligned} \bar{u} U_1 + (\bar{\tau}_1 - \bar{x}) U_2 + \bar{\sigma}_1 U_3 + \bar{\sigma}_2 U_4 &= 0, \\ \bar{v} U_1 + \bar{\sigma}_1 U_2 + (\bar{\tau}_2 - \bar{x}) U_3 + \bar{\sigma}_3 U_4 &= 0, \\ \bar{w} U_1 + \bar{\sigma}_2 U_2 + \bar{\sigma}_3 U_3 + (\bar{\tau}_3 - \bar{x}) U_4 &= 0. \end{aligned} \quad (\text{F10})$$

These can be solved in the $|x|^2 \mapsto \infty$ limit as

$$U_1 \mapsto 1; \quad U_2 \mapsto \frac{x\bar{u}}{|x|^2}; \quad U_3 \mapsto \frac{x\bar{v}}{|x|^2}; \quad U_4 \mapsto \frac{x\bar{w}}{|x|^2}. \quad (\text{F11})$$

We can continue to calculate the potential as in the previous cases. Using the method in Appendix D, analogously to the discussion for two instantons in Appendix E 2 we get

$$\begin{aligned} \mathcal{V} &= 8\pi^2 (|\mathbf{q}|^2 (|u|^2 + |v|^2 + |w|^2) \\ &\quad - 2a\text{Re}_{\mathbb{H}}(\bar{v} \mathbf{q} u) - 2b\text{Re}_{\mathbb{H}}(\bar{u} \mathbf{q} w) - 2c\text{Re}_{\mathbb{H}}(\bar{w} \mathbf{q} v)), \end{aligned} \quad (\text{F12})$$

with a , b , and c given as above.

3. $O(3)$ metric

The final thing to calculate is the metric. As in the previous case, we need to calculate $a^T \delta C_r$, and impose the condition

$$a^T \delta C_r = (a^T \delta C_r)^{T*}. \quad (\text{F13})$$

Note that here we have the operation T rather than \dagger as we are dealing with the usual, real quaternions rather than the complexified version. Since in this commutative

three-instanton case, the remaining symmetry is $o(3)$, we can write

$$\delta R = \begin{bmatrix} 0 & -d\phi & d\theta \\ d\phi & 0 & -d\psi \\ -d\theta & d\psi & 0 \end{bmatrix}. \quad (\text{F14})$$

We should end up, analogously to the previous case, with three simultaneous equations. We now follow the same method as before in Appendixes C and E 3. The solution is

$$\begin{aligned} d\phi &= \frac{1}{\Xi} (D_1(M_{A_2}M_{A_3} + \Psi_3^2) + D_2(M_{A_3}\Psi_1 - \Psi_2\Psi_3) - D_3(M_{A_2}\Psi_2 + \Psi_1\Psi_3)), \\ d\theta &= \frac{1}{\Xi} (-D_1(M_{A_3}\Psi_1 + \Psi_2\Psi_3) - D_2(M_{A_1}M_{A_3} - \Psi_2^2) + D_3(M_{A_1}\Psi_3 + \Psi_1\Psi_2)), \\ d\psi &= \frac{1}{\Xi} (D_1(\Psi_1\Psi_3 - M_{A_2}\Psi_2) + D_2(M_{A_1}\Psi_3 - \Psi_1\Psi_2) + D_3(M_{A_1}M_{A_2} - \Psi_1^2)), \end{aligned} \quad (\text{F15})$$

where

$$\begin{aligned} D_1 &= \bar{u}dv - \bar{v}du + \bar{\tau}_1 d\sigma_1 - \bar{\sigma}_1 d\tau_1 + \bar{\sigma}_1 d\tau_2 - \bar{\tau}_2 d\sigma_1 + \bar{\sigma}_2 d\sigma_3 - \bar{\sigma}_3 d\sigma_2, \\ D_2 &= \bar{u}dw - \bar{w}du + \bar{\tau}_1 d\sigma_2 - \bar{\sigma}_2 d\tau_1 + \bar{\sigma}_1 d\sigma_3 - \bar{\sigma}_3 d\sigma_1 + \bar{\sigma}_2 d\tau_3 - \bar{\tau}_3 d\sigma_2, \\ D_3 &= \bar{v}dw - \bar{w}dv + \bar{\sigma}_1 d\sigma_2 - \bar{\sigma}_2 d\sigma_1 + \bar{\tau}_2 d\sigma_3 - \bar{\sigma}_3 d\tau_2 + \bar{\sigma}_3 d\tau_3 - \bar{\tau}_3 d\sigma_3, \\ M_{A_1} &= |u|^2 + |v|^2 + 3|\sigma_1|^2 + \Sigma^2 + |\tau_1 - \tau_2|^2, \\ M_{A_2} &= |w|^2 + |v|^2 + 3|\sigma_2|^2 + \Sigma^2 + |\tau_1 - \tau_3|^2, \\ M_{A_3} &= |w|^2 + |v|^2 + 3|\sigma_3|^2 + \Sigma^2 + |\tau_2 - \tau_3|^2, \\ \Psi_1 &= \text{Re}_{\mathbb{H}}(3(\bar{\tau}_1\sigma_3 - \bar{\sigma}_2\sigma_1) - \bar{w}v), \\ \Psi_2 &= \text{Re}_{\mathbb{H}}(3(\bar{\tau}_2\sigma_2 - \bar{\sigma}_1\sigma_3) - \bar{u}w), \\ \Psi_3 &= \text{Re}_{\mathbb{H}}(3(\bar{\tau}_3\sigma_1 - \bar{\sigma}_3\sigma_2) - \bar{v}u), \\ \Xi &= M_{A_1}M_{A_2}M_{A_3} + M_{A_1}\Psi_3^2 - M_{A_2}\Psi_2^2 - M_{A_3}\Psi_1^2. \end{aligned} \quad (\text{F16})$$

Once more we use our formula, modified for real quaternions

$$ds^2 = ds_1^2 + ds_2^2 = 2\pi^2(\text{Tr}^*(2d\Lambda^\dagger d\Lambda + d\Omega^\dagger d\Omega) + \text{Tr}^*((a^\dagger da - (a^\dagger da)^T)dR)), \quad (\text{F17})$$

which enables us to calculate the metric as

$$ds^2 = 8\pi^2(d^2u + d^2v + d^2w + d^2\tau_1 + d^2\tau_2 + d^2\tau_3 + d^2\sigma_1 + d^2\sigma_2 + d^2\sigma_3 - (D_1d\phi + D_2d\theta + D_3d\psi))^2. \quad (\text{F18})$$

-
- [1] A. A. Belavin, A. M. Polyakov, A. S. Schwartz, and Yu. S. Tyupkin, Pseudoparticle solutions of the yang-mills equations, *Phys. Lett.* **59B**, 85 (1975).
 [2] M. F. Atiyah, N. J. Hitchin, V. G. Drinfeld, and Yu. I. Manin, Construction of instantons, *Phys. Lett.* **65A**, 185 (1978).

- [3] E. Witten, Small instantons in string theory, *Nucl. Phys.* **B460**, 541 (1996).
 [4] D. Tong, Tasi lectures on solitons: Instantons, monopoles, vortices and kinks, in Theoretical Advanced Study Institute in Elementary Particle Physics: Many Dimensions of String

- Theory (TASI 2005) Boulder, Colorado, 2005 (2005), [arXiv:hep-th/0509216](https://arxiv.org/abs/hep-th/0509216).
- [5] N. D. Lambert and D. Tong, Dyonic instantons in five-dimensional gauge theories, *Phys. Lett. B* **462**, 89 (1999).
- [6] K. Peeters and M. Zamaklar, Motion on moduli spaces with potentials, *J. High Energy Phys.* **12** (2001) 032.
- [7] O. Aharony, M. Berkooz, S. Kachru, N. Seiberg, and E. Silverstein, Matrix description of interacting theories in six dimensions, *Adv. Theor. Math. Phys.* **1**, 148 (1997).
- [8] O. Aharony, M. Berkooz, and N. Seiberg, Light cone description of (2,0) superconformal field theories in six-dimensions, *Adv. Theor. Math. Phys.* **2**, 119 (1998).
- [9] M. Douglas, On $d = 5$ super Yang-Mills theory and (2,0) theory, *J. High Energy Phys.* **02** (2011) 011.
- [10] N. Lambert, C. Papageorgakis, and M. Schmidt-Sommerfeld, M5-branes, d4-branes and quantum 5d super-Yang-Mills, *J. High Energy Phys.* **01** (2011) 083.
- [11] N. S. Manton, A remark on the scattering of BPS monopoles, *Phys. Lett.* **110B**, 54 (1982).
- [12] N. Dorey, T. J. Hollowood, V. V. Khoze, and M. P. Mattis, The calculus of many instantons, *Phys. Rep.* **371**, 231 (2002).
- [13] J. P. Allen and D. J. Smith, The low energy dynamics of charge two dyonic instantons, *J. High Energy Phys.* **02** (2013) 113.
- [14] A. Iskauskas and D. J. Smith, Moduli space dynamics of noncommutative u(2) instantons, *J. High Energy Phys.* **06** (2015) 036.
- [15] E. Hitzer, Introduction to clifford's geometric algebra, *J. Soc. Instrum. Control Eng.* **51**, 338 (2012).
- [16] A. K. M. R. Francis, The construction of spinors in geometric algebra, *Ann. Phys. (Amsterdam)* **317**, 383 (2005).
- [17] N. Nekrasov and A. S. Schwarz, Instantons on noncommutative r^{*4} and (2,0) superconformal six-dimensional theory, *Commun. Math. Phys.* **198**, 689 (1998).
- [18] D. Bak and A. Gustavsson, One dyonic instanton in 5d maximal sym theory, *J. High Energy Phys.* **07** (2013) 021.
- [19] D. H. Correa, G. S. Lozano, E. F. Moreno, and F. A. Schaposnik, Comments on the u(2) noncommutative instanton, *Phys. Lett. B* **515**, 206 (2001).
- [20] C.-S. Chu, V. V. Khoze, and G. Travaglini, Notes on noncommutative instantons, *Nucl. Phys.* **B621**, 101 (2002).
- [21] J. E. Moyal, Quantum mechanics as a statistical theory, *Proc. Cambridge Philos. Soc.* **45**, 99 (1949).
- [22] R. Gopakumar, S. Minwalla, and A. Strominger, Non-commutative solitons, *J. High Energy Phys.* **05** (2000) 020.
- [23] N. Manton and P. Sutcliffe, *Topological Solitons* (Cambridge University Press, Cambridge, England, 2004).
- [24] N. Dorey, V. V. Khoze, and M. P. Mattis, Multi—instanton calculus in $n = 2$ supersymmetric gauge theory, *Phys. Rev. D* **54**, 2921 (1996).
- [25] E. J. Weinberg and P. Yi, Magnetic monopole dynamics, supersymmetry, and duality, *Phys. Rep.* **438**, 65 (2007).
- [26] N. A. Nekrasov, Noncommutative instantons revisited, *Commun. Math. Phys.* **241**, 143 (2003).
- [27] C. Furey, Standard model physics from an algebra?, Ph.D. thesis, Waterloo University, 2015, <https://www.repository.cam.ac.uk/bitstream/handle/1810/254719/Furey-2015-PhD.pdf?sequence=4>.
- [28] A. Cockburn, Aspects of vortices and hyperbolic monopoles, Ph.D. thesis, University of Durham, 2015, <http://etheses.dur.ac.uk/11107/>.
- [29] E. Witten, Constraints on supersymmetry breaking, *Nucl. Phys.* **B202**, 253 (1982).
- [30] P. Yi and M. Stern, Counting Yang-Mills dyons with index theorems, *Phys. Rev. D* **62**, 125006 (2000).
- [31] H.-C. Kim, S. Kim, E. Koh, K. Lee, and S. Lee, On instantons as Kaluza-Klein modes of M5-branes, *J. High Energy Phys.* **12** (2011) 031.
- [32] N. Lambert, C. Papageorgakis, and M. Schmidt-Sommerfeld, Deconstructing (2,0) proposals, *Phys. Rev. D* **88** (2013).
- [33] H. Osborn, Semiclassical functional integrals for selfdual gauge fields, *Ann. Phys. (N.Y.)* **135**, 373 (1981).